General Disclaimer

One or more of the Following Statements may affect this Document

- This document has been reproduced from the best copy furnished by the organizational source. It is being released in the interest of making available as much information as possible.

- This document may contain data, which exceeds the sheet parameters. It was furnished in this condition by the organizational source and is the best copy available.

- This document may contain tone-on-tone or color graphs, charts and/or pictures, which have been reproduced in black and white.

- This document is paginated as submitted by the original source.

- Portions of this document are not fully legible due to the historical nature of some of the material. However, it is the best reproduction available from the original submission.

CSC/SD-75/6020

MATHEMATICAL FORMULATION OF THE APPLICATIONS TECHNOLOGY SATELLITE-F (ATS-F) ORBITAL MANEUVER CONTROL PROGRAM (CNTRLF)

Prepared For

NATIONAL AERONAUTICS AND SPACE ADMINISTRATION

Goddard Space Flight Center

Greenbelt, Maryland

CONTRACT NAS 5-11999

Task Assignment 304

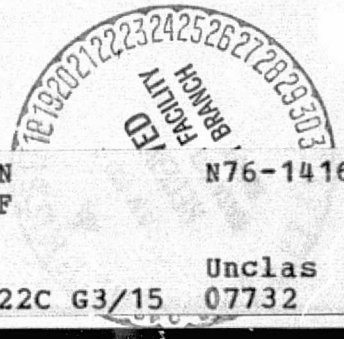

JULY 1975

CSC

COMPUTER SCIENCES CORPORATION

ABSTRACT

This document presents the mathematical formulation of CNTRLF, the maneuver control program for the Applications Technology Satellite-F (ATS-F). The purpose of the document is to specify the mathematical models that are included in the design of CNTRLF. It serves as final documentation, superseding the preliminary Mathematical and Programming Task Specifications for the ATS-F Orbital Maneuver Control Program (CNTRLF).

TABLE OF CONTENTS

LIST OF ILLUSTRATIONS

Figure

LIST OF TABLES

Table

SECTION 1 - INTRODUCTION

This document specifies the mathematical models that are included in the design of CNTRLF--the maneuver control program for the Applications Technology Satellite-6 (ATS-6).[1] Also, the ATS-6 maneuver control hardware and maneuver requirements are summarized to identify the control system characteristics which were modeled.

To satisfy the specific requirements of different audiences, CNTRLF is documented in several volumes. The Mathematical and Programming Task Specification for the ATS-F Orbital Maneuver Control Program (CNTRLF) (Reference 1) describes the preliminary functional requirements and design of CNTRLF. It provides the analyst and programmer with the background material needed to understand the evolution of CNTRLF. The Subsystem Description for the Applications Technology Satellite-F (ATS-F) Orbital Maneuver Control Program (CNTRLF) (Reference 2) contains the details of the CNTRLF design and is directed toward programming and maintenance personnel. The User's Manual for the ATS-F Orbital Maneuver Control Program (CNTRLF) (Reference 3) is directed toward a general audience of analysts, programmers, and data technicians. In addition to a brief description of the program, the principal contents of the User's Manual are descriptions of the specific requirements for data card input to the program.

This document is final documentation and supersedes Reference 1. It serves as an introduction to CNTRLF for programmers who must maintain and enhance the CNTRLF program. It is most helpful also for the analyst who must be familiar with the program at the algorithm level.

---

[1] ATS-F was renamed ATS-6 after its launch in May 1974. For consistency, ATS-6 will be used throughout the remainder of the document.

1.1 HISTORICAL BACKGROUND

Originally, design of the orbital maneuver control program for ATS-6 was to be based on the existing program for ATS series spacecraft (CONTRL). Reference 1 discusses this design based on modifications to the CONTRL program. The principal modifications to CONTRL included: the calculation of the thrust vector direction; the calculation of the change in magnitude of the velocity vector (ΔV) for drift rate and inclination corrections; the calculation of the propulsion system operating state during burns; the prediction of orbital changes resulting from ion engine operation; and the elimination of computations required for attitude maneuvers. Early in the implementation of this design it became evident that the ATS-6 control problem was much more unique than originally envisioned. The scope of the modifications required to accommodate the difference between the stabilization and propulsion subsystem of ATS-6 and the operational ATS-1 and -3 warranted changes to the original design.

In a parallel effort, the structure of the Synchronous Meteorological Satellite (SMS) maneuver control program (SMSMAN) (Reference 4) was being developed. SMSMAN, a generalized maneuver control program for spin-stabilized satellites contained many of the features required in the design of CNTRLF. Therefore, rather than modifying CONTRL to support ATS-6, the SMSMAN program was chosen as the base program.

The CNTRLF program is being used operationally to compute orbital adjust maneuvers for ATS-6. The original design has been updated to include station-keeping logic, node change maneuver logic, an improved method for calculating the drift rate, a hydrazine engine propulsion model, a finite burn integration model, and an improved internal orbit generator.

1.2 ATS-6 SPACECRAFT DESIGN FOR PERFORMING ORBITAL ADJUST MANEUVERS

Orbital adjust maneuvers as well as certain attitude control functions for ATS-6 are performed with the Spacecraft Propulsion System (SPS). Two experimental ion engines are available for supplementary inclination and node corrections. The SPS uses a hydrazine (N_2H_4) thrusting system, consisting of 2 fuel tanks pressurized by gaseous nitrogen (N_2) and 16 heated thrusters. The SPS is completely redundant, and fuel from either tank may be directed to any nozzle by switching the latching valves incorporated in the fuel lines. The location and thrusting direction, with respect to the spacecraft's X, Y, and Z axes, of each of the SPS thrusters is known. Figure 1-1 shows the configuration of the thrusters on the orbital control jets (OCJ) bar. Thrusters 7, 8, 15, and 16 are dedicated solely to east-west orbital maneuvering. Thrusters 13 and 5 and thrusters 14 and 6 are used in pairs to control the north-south orbital maneuvering.

The two ion engines are mounted with their thrust axes nominally at ±45 degrees from the spacecraft's +Z-axis in the Y-Z plane as illustrated in Figure 1-2. In general, the thrusters are positioned so that their thrust acts through the center of gravity. However, some torque will be placed on the spacecraft due to changing fuel levels and initial misalignments.

1.2.1 Orbital Maneuvers With the SPS

The SPS provides thrust to change the orbital velocity of the spacecraft for east-west and north-south orbit control. The SPS also provides thrust to torque the spacecraft about its axes for attitude control. The basic orbital maneuvers scheduled to be performed by the SPS for ATS-6 are initial station acquisition, east-west stationkeeping at 94 degrees west and 35 degrees east longitude, a transfer from 94 degrees west to 35 degrees east longitude (India) and the return to 105 degrees west longitude, and north-south stationkeeping as needed.

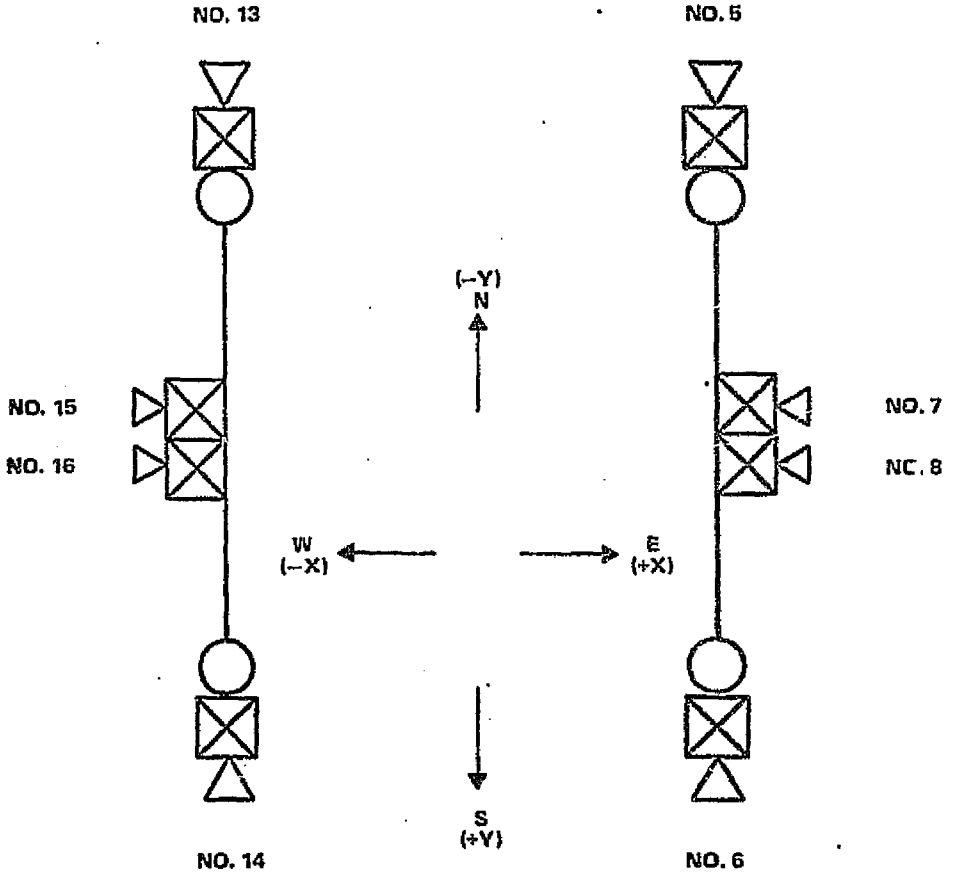

Figure 1-1. Alternate Orbital Control Jets (OCJ) Bar Thruster Configuration

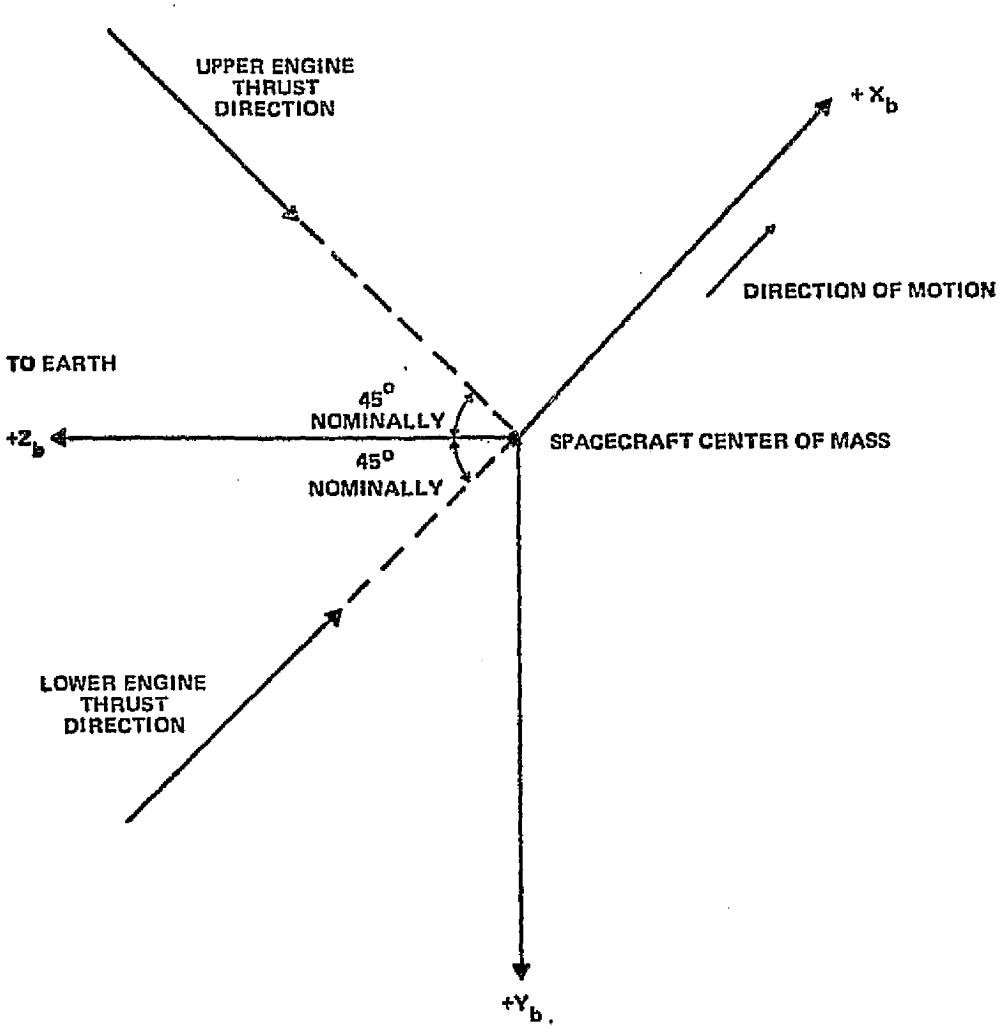

Figure 1-2. Ion Engine Thrust Vector Geometry Relative to Spacecraft Axes

The continuous mode of thruster operations is used for all orbit control functions of the spacecraft. In this mode, thruster ON times range from 1.0 second to approximately 6 hours. The OFF time durations generally range from hours to days or months, so that each start is considered to occur at the ambient hardware temperature. The other mode of operation is the pulse mode. This mode is used almost exclusively for attitude control functions on the spacecraft. It is generally characterized by very short ON times (.10 second (100 milliseconds) to 120 seconds), with relatively long OFF times (10 seconds to days). When orbital maneuvers are being performed, the Attitude Control System (ACS) stabilizes the spacecraft in the jet only mode. Attitude is maintained by the attitude thrusters, and momentum wheels are not used for reaction torquing.

As stated earlier, the orbital thrusting produces torques. Hence, it is not unlikely for an attitude thruster to fire in the pulse mode during an orbital maneuver. Thus, if thruster 7 is being used for a normal east-west stationkeeping maneuver, thruster 3 or 11 (the pitch thruster) may be fired in pulsed bursts to correct errors in pitch. The perturbations of the orbital elements arising from the attitude reaction thruster during orbital maneuvers have been estimated to be less than 1 percent of the desired maneuver. By deliberately misaligning the orbital thrusters, the thrust produced by the attitude thrusters will aid in accomplishing the desired maneuver.

Figure 1-3 contains the nominal SPS performance data as a function of tank pressure. The data were reduced from tests conducted during the qualification and acceptance test phase. Appendix A contains a more detailed analysis of SPS performance characteristics.

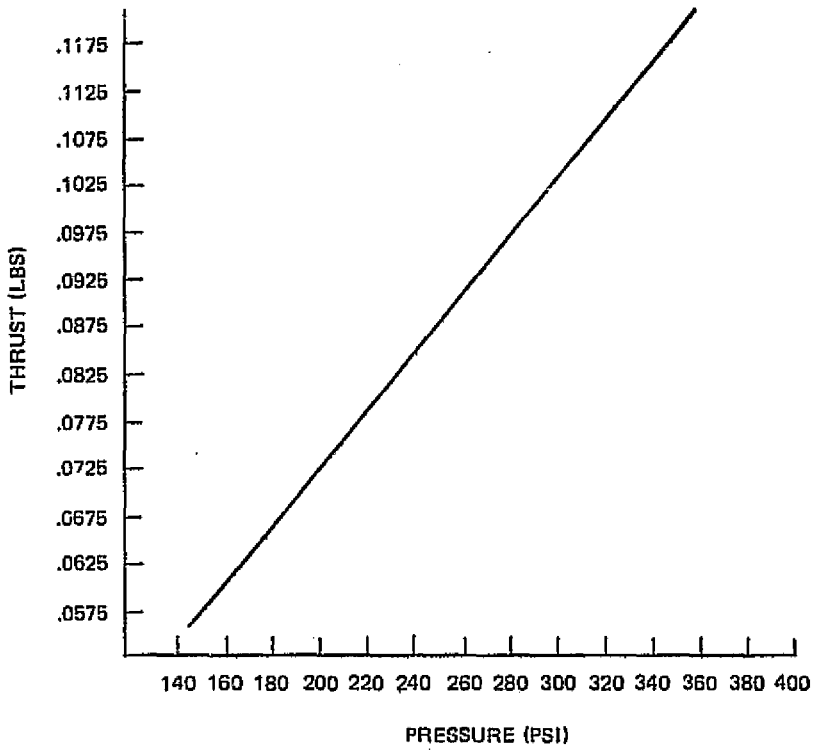

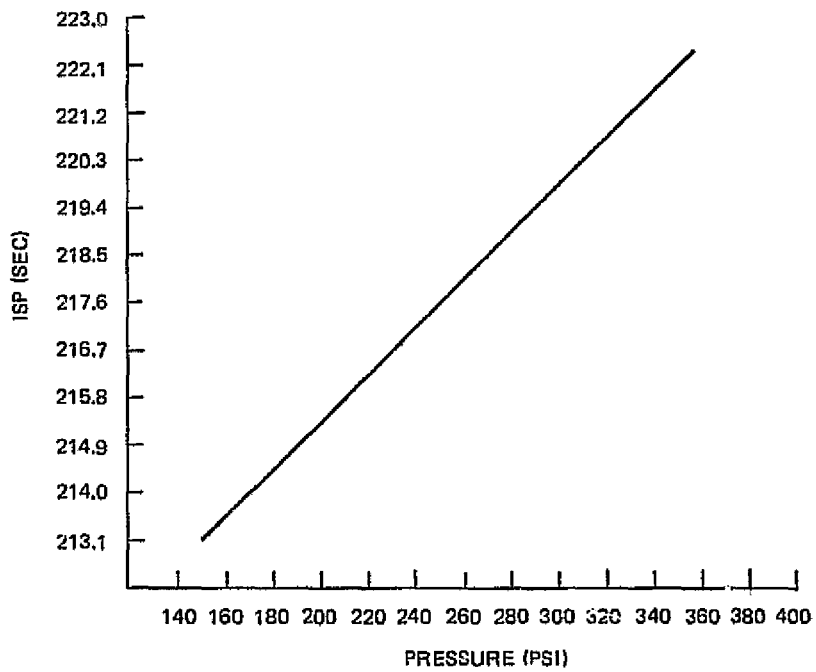

Figure 1-3. Thruster Model at 70°

1.2.2 Orbital Maneuvers With the Ion Engines

The ATS-6 spacecraft carries two identical Cesium bombardment ion engines for experimental use in making inclination and node corrections. Upon command, the engines can deflect the thrust vector direction ±7 degrees from the nominal direction. Thus, the ion engines can be positioned to thrust through the center of gravity. It is planned that the duty cycle during the ion engine experiment will be 7 hours of continuous operation for each 12-hour interval centered at the nodal crossings, covering a 1-month period. The thrust level of the ion engines is on the order of 0.001 pound force, and the specific impulse is approximately 2500 seconds.

1.3 FUNCTIONAL SPECIFICATIONS FOR CNTRLF

The original functional specifications for CNTRLF were written in June 1972. These specifications were addressed in Reference 1. As a result of the decision to use SMSMAN as a base program instead of CONTRL, new functional specifications were written. In this section the new specifications are given as a reference to the reader.

CNTRLF will compute maneuver control data for orbital and stationkeeping maneuvers to be performed by the ATS-6 spacecraft. It will be an offline program designed for use on the IBM 360 computers at the Goddard Space Flight Center (GSFC) and will be written in the FORTRAN IV language.

Maneuver control data will be computed for the following SPS maneuvers: initial orbit correction, east-west stationkeeping (at 94 degrees west, 35 degrees east longitude), the transfer to India and the return, and north-south stationkeeping. Maneuver control data will be computed also for the north-south stationkeeping maneuvers for the ion engine experiment.

It will be possible to compute maneuvers in any one of four possible attitude configurations--reference, 3-axis, spin and Sun.

1. Reference--This will be the normal operational attitude mode for the spacecraft when orbital maneuvers are being performed. Input attitude data will not be required. The program will compute the current attitude during the maneuver.

2. 3-Axis--The three Euler angle rotations (yaw, roll, and pitch) will be entered and will remain constant throughout the computations.

3. Spin--This option will be used during initial acquisition (launch mode) when the spacecraft is spinning about its X-axis. The right ascension and declination of the spin axis will be the input data used to describe attitude. The attitude in inertial coordinates will be held fixed throughout the computations. Due to thruster orientation, only east-west maneuvers will be computed in this attitude mode.

4. Sun--This option, like the spin option, will be used only during initial acquisition when the spacecraft's X-axis is known to be aligned with and spinning about the Sun line. The input to CNTRLF will consist of the time of this alignment. The Sun declination and right ascension will be known a priori. The orientation of the ATS-6 spin axis will be set to the values at Sun sighting.

The following models will be internal to CNTRLF:

1. Hydrazine engine propulsion model
2. Ion engine thrust perturbation model
3. Finite burn integration model (fourth-order Adams-Moulton)

The CNTRLF program will be able to operate using the following sources of orbit data:

1. Tape or disk input (ORB1, EPHEM, GTDS sequential orbit file)
2. Disk input (GTDS ORBIT file)
3. Internal orbit generator (BPACKT/BPACKC)

Card input to the program will contain the following information:

1. Initial spacecraft attitude
2. Initial spacecraft orbit source and data, if necessary
3. Desired maneuver
4. Desired time to perform maneuver
5. Engine to be used
6. Engine and fuel tank initial states
7. Current engine calibration factors

Program output (line printer) will contain the following information:

1. Input card images
2. Input summary
3. Propulsion system table
4. Orbit and drift table
5. Maneuver summary
6. Control sheet
7. Appropriate error messages

The program will make the following nonrestrictive assumptions:

1. Operating configuration parameters will not be specified (e.g., heater turn-on times, latching value settings, coding of commands).
2. The flight system data will be averaged into a homogeneous thruster model. This single model will contain thrust and specific impulse (ISP) data as a function of pressure, time, and temperature. A calibration factor will be used to adjust the homogeneous model for a specific thruster.
3. The internal program models will neglect the effect of attitude thrusting during orbital maneuvers. The effect will be included by proper adjustment of the thruster calibration factors.

4. The reference time will be Greenwich Mean Time (GMT).

5. Engine cool down will not be modeled; thus, every burn will proceed as if the engine started at the ambient temperature.

SECTION 2 - MATHEMATICAL MODELS

The mathematical models included in the CNTRLF program are described in this section according to the following categories:

1. Orbital element systems
2. Coordinate systems
3. Maneuver options
4. Hydrazine engine propulsion model
5. Finite burn integration model (fourth-order Adams-Moulton)
6. Ion engine thrust perturbation model
7. Orbit sources before the burn

No attempt is made to show how the models are integrated to obtain a working program. Reference 3 contains the necessary information on program structure and interfaces.

2.1 ORBITAL ELEMENTS

The spacecraft orbit is specified by one of the following sets of generalized coordinates:

1. Inertial position and velocity vectors
2. Osculating Keplerian elements
3. Injection or flight parameters
4. Mean osculating elements

2.1.1 Inertial Position and Velocity Vectors

The inertial position and velocity vectors are defined as follows:

$\vec{R} = (X , Y , Z)$ = the position or radius vector of the spacecraft from the center of the Earth expressed in the inertial coordinate system

$\vec{V} = (\dot{X} , \dot{Y} , \dot{Z})$ = the velocity vector of the spacecraft expressed in the inertial coordinate system

The usual units of $\vec{R}$ and $\vec{V}$ components are Earth radial units (ERU) and ERU per second, respectively. One ERU equals the average radius of the Earth, or 6378.140 kilometers.

2.1.2 Osculating Keplerian Elements

The osculating Keplerian elements are defined as follows:

- a = semimajor axis
- e = eccentricity
- i = inclination
- m = mean anomaly
- ω = argument of perigee
- Ω = right ascension of the ascending node

The usual set of units for osculating Keplerian elements are either a in kilometers, e dimensionless, and i , m , ω , Ω in degrees; or a in ERU, e dimensionless, and i , m , ω , Ω in radians. Figure 2-1 illustrates four of these elements.

2.1.3 Injection or Flight Parameters

The injection or flight parameters are defined as follows:

- ϕ = geodetic latitude of spacecraft subsatellite point in degrees (measured positive for north latitude)
- λ = longitude of spacecraft subsatellite point in degrees (measured positive for longitude west of Greenwich)
- r = magnitude of the spacecraft radius vector in nautical miles
- v = magnitude of the spacecraft velocity vector in feet per second
- γ = flight path elevation angle; the elevation of the inertial velocity vector in degrees (measured positive outward from the plane perpendicular to the radius vector)

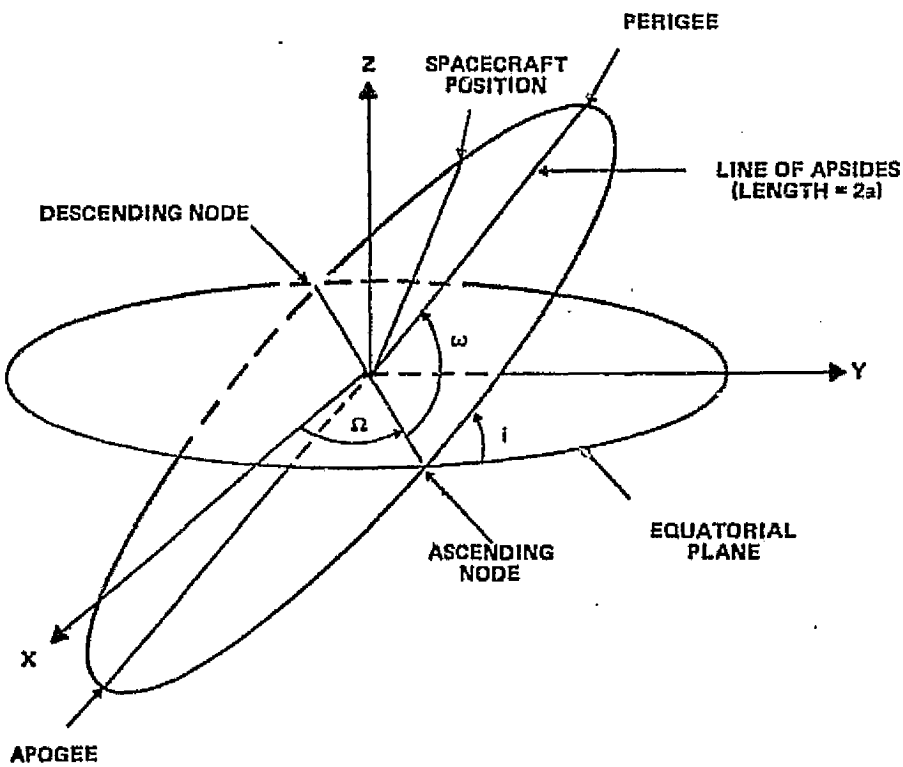

Figure 2-1. Osculating Keplerian Elements

α = flight path azimuth angle; the azimuth of the inertial velocity vector projection onto the plane perpendicular to the radius vector in degrees (measured positive clockwise from east)

Figure 2-2 illustrates these parameters.

2.1.4 Mean Osculating Elements

The mean osculating elements are used in Brouwer theory as an intermediate step in propagating the orbit. For details concerning mean elements, see Reference 5.

2.1.5 Orbital Element Conversion

Standard conversion formulas exist to convert elements of one system to those of another (Reference 6). These formulas have been programmed into a standard set of software (Reference 5) which is used in many of the operational programs at GSFC. Both CNTRLF and SMSMAN have combined these routines into a single package. This reduces the conversion task to a single call to a main driver. Subroutine ELMNT is used as a main driver of the standard conversion subroutines. The existing and the desired element types are each specified through ELEMNTs argument list by one of the following alphameric names: INERTIAL for inertial position and velocity vectors; OSCULATE for osculating Keplerian elements; INJECTION for injection parameters; and MEAN for Brouwer mean osculating elements. Thus, if the input parameter is INERTIAL and the output name is OSCULATE, ELEMNT calls those standard routines which will convert inertial position and velocity vectors to osculating Keplerian elements.

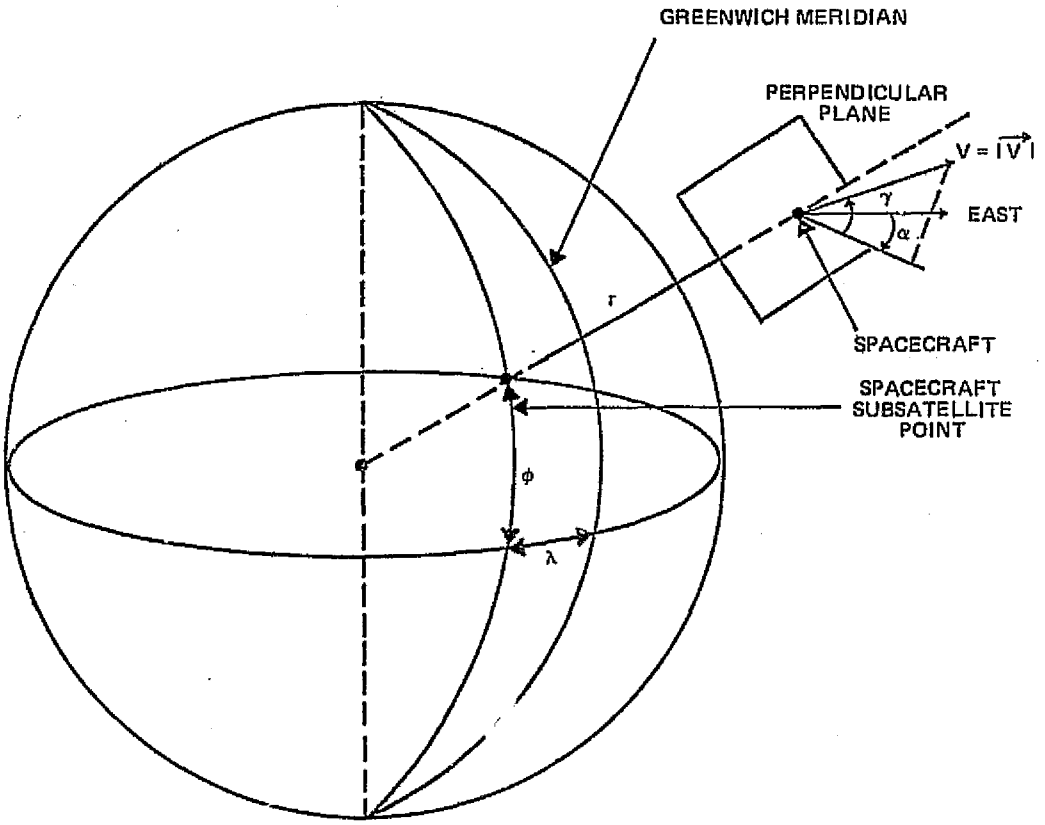

Figure 2-2. Injection Parameters

2.2 COORDINATE SYSTEMS

The Earth-centered inertial (ECI) reference frame is defined by the following set of unit vectors:

$\hat{i}_i$ = direction of mean equinox of date
$\hat{j}_i = \hat{k}_i \times \hat{i}_i$
$\hat{k}_i$ = direction of north celestial pole

When the SPS or ion engines are to be used for orbital maneuvers, the direction of the ΔV vector or the thrust vector must be computed in the ECI frame. The unit vector obtained will be changing slowly as the spacecraft maintains a 3-axis stabilized condition, pointing at a location on the Earth.

The calculation of the thrust vector in the ECI frame is done in a two-step process. First, the direction of thrust is transformed from the spacecraft body axis frame to the local vertical (LV) frame (see Section 2.2.1). The second transformation is from the LV frame to the ECI frame (see Section 2.2.2).

The spacecraft body axis frame is defined by the following unit vectors (see Figure 2-3):

$\hat{i}_b = \hat{j}_b \times \hat{k}_b$
$\hat{j}_b$ = parallel to mounting axis of solar array panel and positively directed away from optical axis of Polaris sensor
$\hat{k}_b$ = through center of parabolic reflector and center of Earth-viewing module; assumed positive in that direction

The LV reference frame is defined by the following unit vectors (see Figure 2-3):

$\hat{i}_{LV}$ = east, parallel with the equatorial plane
$\hat{j}_{LV} = \hat{k}_{LV} \times \hat{i}_{LV}$, nominally south
$\hat{k}_{LV}$ = down, through the Earth's center of mass

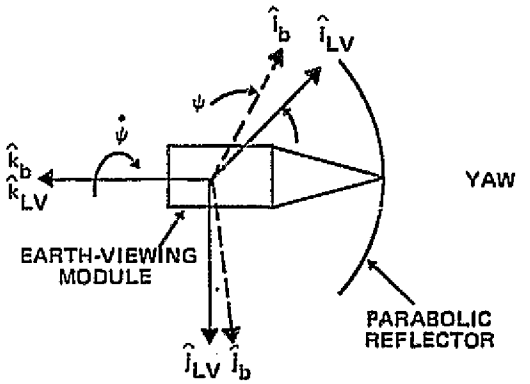

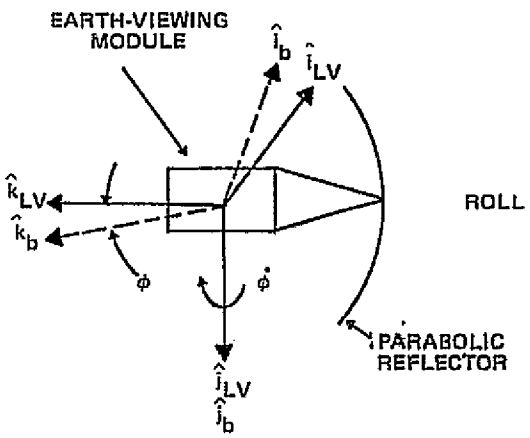

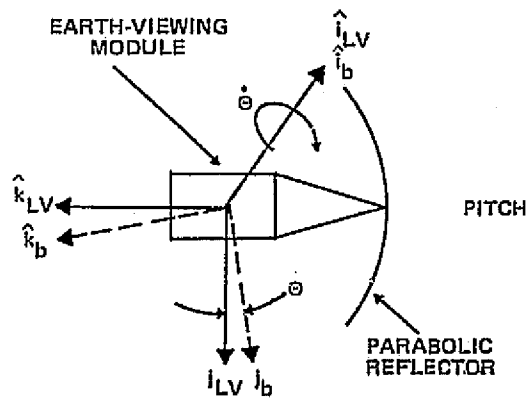

Figure 2-3. Euler Rotation From Body Frame to LV Frame

Table 2-1 gives the body coordinates for the SPS thrusters and ion engines aboard ATS-6. Note that the east-west thrusters are canted, thus introducing a component of thrust away from the Earth for both eastward and westward thrusting. The cant angle has a magnitude of 5.575 degrees. The ion engines are mounted on a pivot and are movable by command from the ground. The angle between the spacecraft's Z-axis and the direction of thrust of the ion engine (C_α) has been included to model this condition.

The transformation from the spacecraft body axis frame to the ECI frame depends on the spacecraft attitude, the spacecraft orbital position, and the direction of the thrust relative to the spacecraft embedded axis. The ATS-6 spacecraft attitude is entered into CNTRLF in one of the following modes (Section 2.2.3):

1. Reference
2. 3-Axis
3. Spin
4. Sun

During the lifetime of ATS-6, it is expected that the above four methods of specifying attitude will cover all possible configurations in which an orbital maneuver could be performed. The user-specified orbit source (see Section 2.7) defines the initial orbit position. Table 2-1 defines the orientation of the thrust vector in the spacecraft body axis. Sections 2.2.1 and 2.2.2 describe the transformation from the spacecraft body axis frame to the ECI frame assuming that the spacecraft attitude, orbital position, and embedded axes have been defined previously. Section 2.2.3 describes the four possible methods of specifying attitude information.

Table 2-1. Body Coordinates for the Orbital Thrusters Onboard AT6-6

AV AND THRUST DIRECTION	THRUSTER NUMBER	THRUST VECTOR COMPONENTS IN BODY AXIS FRAME
HYDRAZINE ENGINE		
NOMINALLY WEST	7 OR 8	$\bar{T}_b = \begin{bmatrix} -\cos \alpha_c \\ 0 \\ -\sin \alpha_c \end{bmatrix}$
NOMINALLY EAST	15 OR 16	$\bar{T}_b = \begin{bmatrix} +\cos \alpha_c \\ 0 \\ -\sin \alpha_c \end{bmatrix}$
NOMINALLY SOUTH	5 AND 13	$\bar{T}_b = \begin{bmatrix} 0 \\ 1 \\ 0 \end{bmatrix}$
NOMINALLY NORTH	6 AND 14	$\bar{T}_b = \begin{bmatrix} 0 \\ -1 \\ 0 \end{bmatrix}$
ION ENGINE		
SOUTH OR NORTH*	NOT APPLICABLE	$\bar{T}_b = \begin{bmatrix} 0 \\ \sin C_\alpha \\ -\cos C_\alpha \end{bmatrix}$

*DEPENDS ON SIGN OF C_α

α_c IS THE EAST-WEST THRUSTERS CANT ANGLE (A CONSTANT VALUE OF 5.575 DEGREES)

C_α IS THE ANGLE THE ION ENGINE MAKES WITH THE SPACECRAFTS Z-AXIS (NOMINALLY $\pm$45 DEGREES)

2.2.1 Transformation From Spacecraft Body Axis Frame to LV Frame

The spacecraft attitude is defined by the following set of three Euler rotations from the spacecraft body system to the LV frame:

1. Yaw angle, ψ
2. Roll angle, ϕ
3. Pitch angle, θ

Figure 2-3 defines each of these individual rotations.

Given the attitude (ψ , ϕ , θ) , the Euler transformation matrix used in the transformation from spacecraft body axis to the LV frame is defined as follows:

$$M = M_{\psi} M_{\phi} M_{\theta}$$

where M_{ψ} is the yaw angle transformation matrix

$$M_{\psi} = \begin{bmatrix} \cos\psi & -\sin\psi & 0 \\ \sin\psi & \cos\psi & 0 \\ 0 & 0 & 1 \end{bmatrix} \qquad (2\text{-}1)$$

M_{ϕ} is the roll angle transformation matrix

$$M_{\phi} = \begin{bmatrix} 1 & 0 & 0 \\ 0 & \cos\phi & -\sin\phi \\ 0 & \sin\phi & \cos\phi \end{bmatrix} \qquad (2\text{-}2)$$

and M_θ is the pitch angle transformation matrix

$$M_\theta = \begin{bmatrix} \cos\theta & 0 & \sin\theta \\ 0 & 1 & 0 \\ -\sin\theta & 0 & \cos\theta \end{bmatrix} \tag{2-3}$$

Solving for M in the pitch, roll, yaw sequence,

$$M = \begin{bmatrix} \cos\psi\cos\theta - \sin\psi\sin\phi\sin\theta & -\sin\psi\cos\phi & \cos\psi\sin\theta + \sin\psi\sin\phi\cos\theta \\ \sin\psi\cos\theta + \cos\psi\sin\phi\sin\theta & \cos\psi\cos\phi & \sin\psi\sin\theta - \cos\psi\sin\phi\cos\theta \\ -\cos\phi\sin\theta & \sin\phi & \cos\phi\cos\theta \end{bmatrix} \tag{2-4}$$

Defining $\hat{T}_\ell$ to be the unit vector in the direction of thrust in the LV frame and $\hat{T}_b$ the unit vector in the direction of thrust in the body axis frame, it follows that

$$\hat{T}_\ell = M\,\hat{T}_b \tag{2-5}$$

2.2.2 Transformation From LV Frame to ECI Frame

The azimuth and the elevation of the spacecraft position in the ECI frame are η_1 and η_2, respectively (Figure 2-4). Defining $\hat{T}_\ell$ to be the unit vector in the direction of thrust in the LV frame and $\hat{T}_i$ to be the unit vector in the direction of thrust in the ECI frame, it follows that

$$\hat{T}_i = M_\eta\,\hat{T}_\ell \tag{2-6}$$

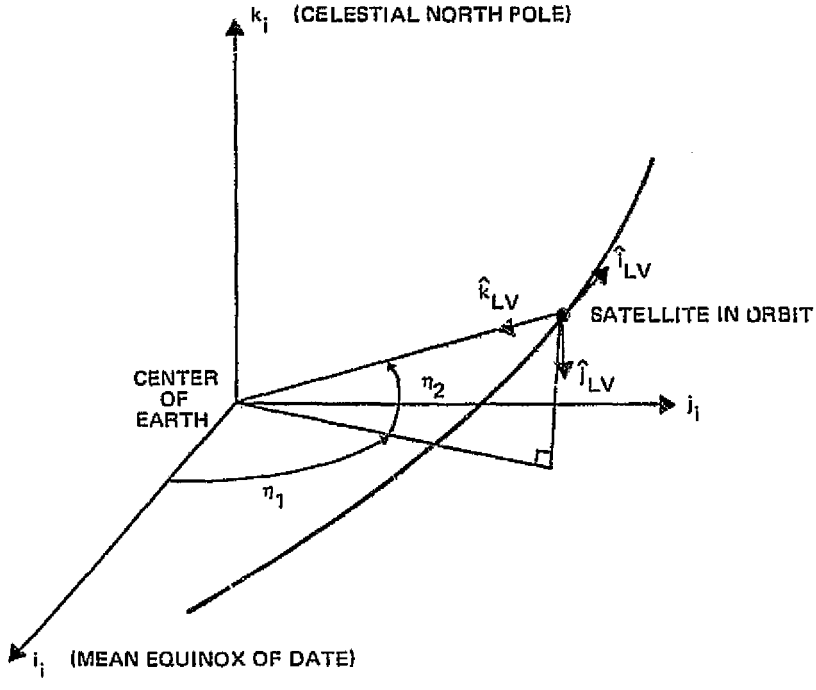

Figure 2-4. Position of Satellite in Inertial Coordinate System

where

$$M_{\eta} = \begin{bmatrix} -\sin \eta_1 & \cos \eta_1 \sin \eta_2 & -\cos \eta_1 \cos \eta_2 \\ \cos \eta_1 & \sin \eta_1 \sin \eta_2 & -\sin \eta_1 \cos \eta_2 \\ 0 & -\cos \eta_2 & -\sin \eta_2 \end{bmatrix} \qquad (2\text{-}7)$$

2.2.3 Modes of Attitude Operation

In the normal mode of orbital thruster operation, the spacecraft attitude is held in the reference mode (Section 2.2.3.1). To model this mode, the program must calculate the three Euler angles (yaw, roll, and pitch) expected during the thrusting period. When the satellite is pointing at a selected station on the Earth, the spacecraft will not be maneuvered into the reference mode. In this mode of operation the three Euler angles will be known a priori, and the angles will be entered as input, using the 3-axis program option (Section 2.2.3.2). During initial acquisition when the spacecraft is spinning about its X-axis and is not 3-axis stabilized, the right ascension and declination of the spin axis will be known directly or could be computed a priori from the time of alignment with the Sun line. If orbital thrusting is requested during this period, CNTRLF will be run in the spin or Sun modes of attitude operations (Sections 2.2.3.3 and 2.3.3.4, respectively).

2.2.3.1 Reference Mode of Operation

This is the normal mode in which attitude is maintained during orbital maneuvers. The Euler angles of roll and pitch are set to zero while the Euler angle of yaw is held so that the thrust vector will be, as closely as possible, either perpendicular or parallel to the orbit velocity vector. If external torques due to the orbital thrusting cause the spacecraft to deviate from this attitude, the appropriate SPS thrusters are fired in the pulsed mode to reduce the error. The Euler angle of yaw is calculated so as to align the spacecraft X-axis as

closely as possible with the orbit velocity vector. Figure 2-5 defines the calculated yaw magnitude. The mathematical models used by the CNTRLF program to compute yaw are:

$$\bar{E} = \begin{bmatrix} -\cos B \\ \sin B \\ 0 \end{bmatrix} \tag{2-8}$$

where $B = \arctan [R_x / R_y]$

R_x = x component of spacecraft position vector in ECI frame

R_y = y component of spacecraft position vector in ECI frame

$$\hat{N} = \frac{\vec{R} \times \vec{V}}{|\bar{R} \times \bar{V}|}$$

$$\hat{T} = \hat{N} \times \hat{R} \tag{2-9}$$

$$\psi = \arccos (\hat{T} \cdot \hat{E})$$

where $\vec{V}$ = satellite velocity vector in the ECI frame

$\vec{N}$ = vector normal to orbit plane in ECI frame

$\vec{T}$ = vector tangential to orbit plane in ECI frame

The three Euler angles are known (yaw = calculated value, roll = 0, pitch = 0) as is the direction of the thrust in the body axis (see Table 2-1). Equation (2-5) is used to calculate the direction of thrust in the LV frame. Knowing the spacecraft position in inertial space, Equation (2-6) is then used to calculate the direction of thrust in the ECI frame.

2.2.3.2 3-Axis Mode of Operation

At times the spacecraft will be tracking an Earth station or low-altitude spacecraft during a time period in which an orbital thrusting maneuver is required.

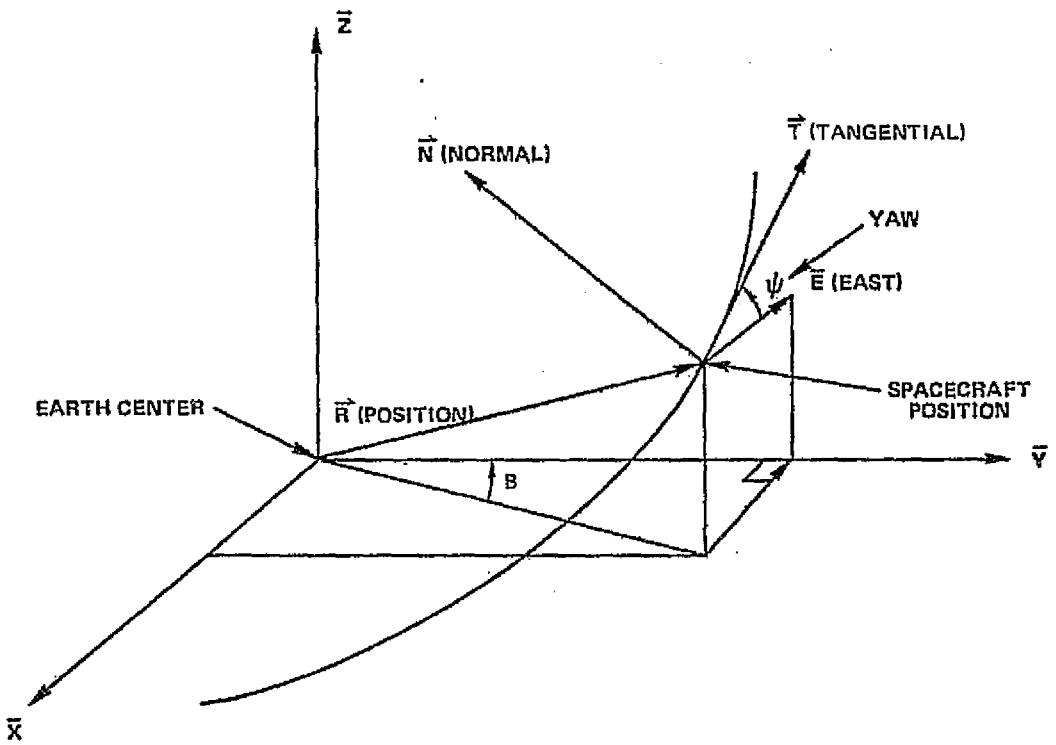

Figure 2-5. Definition of Parameters Used in the Reference Mode

If the three Euler rotations at the desired time of the maneuver are known, they can be entered directly into CNTRLF. The three Euler angles are known (yaw = input, roll = input, pitch = input) as is the direction of the thrust in the body axis (see Table 2-1). Equation (2-5) is used to calculate the direction of thrust in the LV frame. Knowing the spacecraft position in inertial space, Equation (2-6) is then used to calculate the direction of thrust in the ECI frame.

2.2.3.3 Spin Stabilization Mode of Operation

In this mode, the spacecraft is spinning slowly about the axis in which the east-west thrusters (7, 8, 15, and 16) lie (x-axis) and the right ascension and declination of this axis in inertial space is known. Therefore, the direction of thrust in the ECI frame can be solved for directly:

$$\hat{T}_i = \begin{bmatrix} \cos \text{Dec} \cos \text{RA} \\ \cos \text{Dec} \sin \text{RA} \\ \sin \text{Dec} \end{bmatrix} \qquad (2\text{-}10)$$

where $\hat{T}_i$ = the unit vector of thrust for thrusters 15 and 16
(note that $T_i = -T_i$ for thrusters 7 and 8)

Dec = the user-specified spin axis declination

RA = the user-specified spin axis right ascension

2.2.3.4 Sun Stabilization Mode of Operation

In this mode, the spacecraft is known to be aligned with and spinning about the Sun line. The time at which the spacecraft was aligned with the Sun line is entered into the program. A standard ATS routine SUNEPH (see Reference 5) is used to obtain the right ascension and declination of the Sun in inertial space at that time. By using Equation (2-10), the thrust direction in inertial space is computed.

2.3 MANEUVER OPTIONS

In CNTRLF, thrusting requirements are computed for two general types of maneuvers (north-soth and east-west maneuvers). A further breakdown can be made into classes which allow the user to model all orbital maneuvers expected in the lifetime of ATS-6. These classes are:

- North-south maneuvers using the hydrazine thrusters (in pairs) and the ion engine, i.e., inclination change maneuvers, node change maneuvers, and combined inclination and node change maneuvers.
- East-west maneuvers using only the hydrazine thrusters, i.e., drift rate change maneuvers (drift rate goal specified by user) and stationkeeping maneuvers (drift rate goal computed by CNTRLF).

CNTRLF models both north-south and east-west maneuvers in the following manner:

1. Initial estimates of burn time and ignition time are developed
2. The maneuver is modeled step-by-step until the estimated burn time is achieved.
3. It is determined if the desired end conditions have been reached. If they have not, new estimates of burn time and ignition time are developed based on the error. Then, step 2 is repeated.

This section is concerned with the determination of the initial estimates of burn time and ignition time. Those models used in the step-by-step iteration process are discussed in Sections 2.4 through 2.6.

2.3.1 Derivation of ΔV Magnitude for Drift Rate Change Maneuvers

The drift rate goal and the ignition time have been either specified as input or derived as in Section 2.3.3. In either case, the drift rate to be achieved and the current drift rate are known (see Section 2.3.1.1). A change in the drift rate is accomplished by adjusting the semimajor axis of the orbit. A positive

drift rate change (by definition, westward) is achieved by increasing the semi-major axis; a negative drift change (by definition, eastward) is achieved by decreasing the semimajor axis.

The change in the semimajor axis is accomplished by firing one of the east-west thrusters (7, 8, 15, or 16) in the orbit plane. The thrust is divided into a tangential component and a radial component (Figure 2-6). In general, the thrust vector causes a change in both the spacecraft's tangential and radial velocity vectors. Thus, the total change in the velocity vector (ΔV) due to thrusting in the orbit plane is defined as follows:

$$\Delta V = \sqrt{\Delta V_R^2 + \Delta V_T^2} \tag{2-11}$$

where ΔV_R = ΔV component in orbital radial direction

ΔV_T = ΔV component in orbital tangential direction

ΔV = magnitude of ΔV vector

$$\Theta_{\Delta V} = \arctan \frac{\Delta V_T}{\Delta V_R} \tag{2-12}$$

where $\Theta_{\Delta V}$ = angle between ΔV_R and the direction of ΔV

The change in the semimajor axis due to thrusting can be represented by the following Lagrange Planetary equation (Reference 1):

$$\Delta a = \frac{2e \sin f}{\eta\sqrt{1 - e^2}} \Delta V_R + \frac{2a\sqrt{1 - e^2}}{\eta r} \Delta V_T \tag{2-13}$$

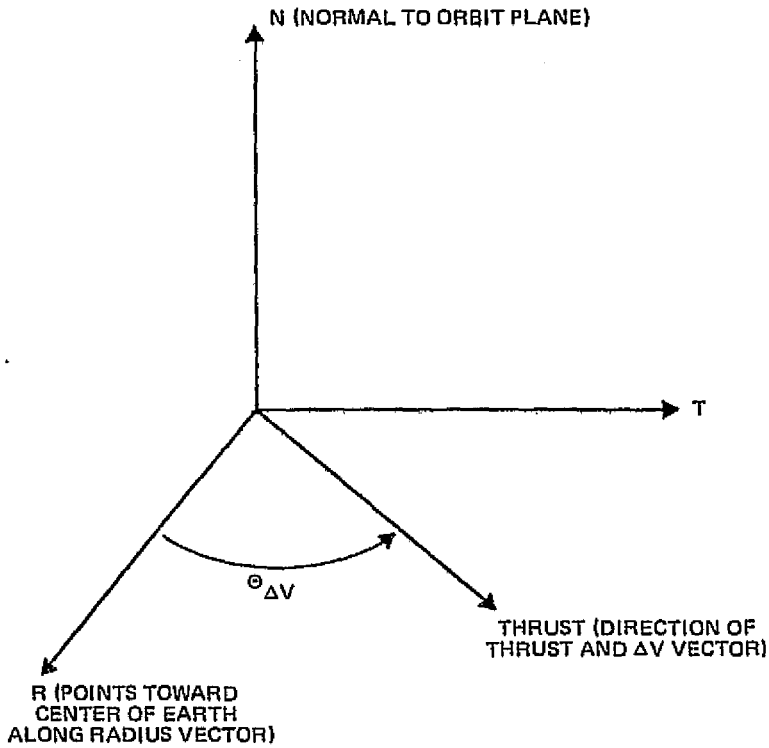

Figure 2-6. Thrust Vector Geometry in East-West Orbital Maneuvers

where Δa = change in semimajor axis (ERU)[1]

f = true anomaly (radians)

a = semimajor axis (ERU)

e = eccentricity (dimensionless)

η = mean motion = $\sqrt{\mu_e/a^3}$ (radians per second)

ΔV_R = thruster velocity component (ΔV) in orbital radial direction

ΔV_T = thruster velocity component (ΔV) in orbital tangential direction

r = position magnitude (ERU)

μ_e = Earth's gravitational constant (62630.01853 ERU^3/sec^2)

The definition for r in elliptic orbits (see Reference 6) is given as

$$r = \frac{a(1 - e^2)}{1 + e \cos f} \tag{2-14}$$

The change in the semimajor axis Δa is also obtained by subtracting the current value of the semimajor axis from the desired value. Both values are calculated from the current and desired drift rates

$$a = \left[\frac{86164.1064\sqrt{\mu_e}}{2\pi\left(1 - \frac{\dot{\lambda}}{360}\right)}\right]^{2/3} \tag{2-15}$$

where a = semimajor axis (ERU)

μ_e = Earth's gravitational constant (62630.01853 ERU^3/sec^2)

$\dot{\lambda}$ = drift rate--either current or desired (degree per day)

where all of the parameters are defined in Equation (2-13).

[1] One ERU = 6378.140 kilometers

Equation (2-13) can be simplified as follows:

$$\Delta a = \frac{2}{\eta\sqrt{1 - e^2}} \left[(e \sin f)\, \Delta V_R + (1 + e \cos f)\, \Delta V_T\right] \tag{2-16}$$

If we define

$$C_1 = \frac{2}{\eta\sqrt{1 - e^2}} e \sin f \tag{2-17}$$

and

$$C_2 = \frac{2}{\eta\sqrt{1 - e^2}} (1 + e \cos f) \tag{2-18}$$

Equation (2-16) can be rewritten as

$$\Delta a = C_1\, \Delta V_R + C_2\, \Delta V_T \tag{2-19}$$

Then, by definition, (see Figure 2-6)

$$\begin{aligned} \Delta V_R &= \Delta V \cos \Theta_{\Delta V} \\ \Delta V_T &= \Delta V \sin \Theta_{\Delta V} \end{aligned} \tag{2-20}$$

Substituting Equation (2-20) into Equation (2-19) and solving for ΔV produces

$$\Delta V = \frac{\Delta a}{C_1 \cos \Theta_{\Delta V} + C_2 \sin \Theta_{\Delta V}} \tag{2-21}$$

2.3.1.1 Drift Rate Algorithm

The accuracy to which the first estimate of ΔV can be calculated depends on how accurately the initial drift rate is known. In CNTRLF, the process for finding the initial drift is the same as that used in the acquisition table generation program for ATS-6, FACTBL (see Reference 7). In FACTBL, 49 subsatellite points, equally spaced in time, are averaged to calculate the average subsatellite longitude over a sidereal day. The drift rate is then calculated by subtracting the current average longitude from the average longitude one sidereal day later. The drift rate and the average longitude are computed in CNTRLF as follows:

$$\dot{\lambda}_i = \lambda av_i - \lambda av_{i+1} \tag{2-22}$$

where $\dot{\lambda}_i$ = initial drift rate in degrees per sidereal day (westward drift is positive)

λav_i , λav_{i+1} = average subsatellite longitudes over a sidereal day at current time and one sidereal day later, respectively (westward longitudes are positive)

$$\lambda av_i = \frac{\lambda_i + \sum_{n=1}^{48} \lambda_{i+(1795.0855n)}}{49} \tag{2-23}$$

where λ_i is the initial subsatellite longitude and $\lambda_{i+(1795.0855n)}$ is the subsatellite longitude at the initial time plus n times 1795.0855 seconds. Both λ_i and $\lambda_{i+(1795.0855n)}$ are calculated by converting the elements from the user-specified orbit source to injection elements (degrees) (see Section 2.1.3).

Once thrusting has started, the position and velocity vectors on the user-specified orbit source are no longer valid. Therefore, the method just described of calculating the drift rate is also no longer valid. The sole orbit

information available after thrusting is that which comes from the finite burn integration model (see Section 2.5). If this derived information is used to calculate λ_i in Equation (2-23) and the orbit is propagated using the internal generator BPACKT (see Reference 11), an expression for drift rate throughout the thrusting period is formed as follows:

$$\dot{\lambda} = \dot{\lambda}_T + (\dot{\lambda}_i - \dot{\lambda}_{ii}) \tag{2-24}$$

where $\dot{\lambda}$ = drift rate after thrusting has started (degrees per sidereal day)

$\dot{\lambda}_T$ = drift rate obtained by propagating the Keplerian osculating elements from the finite burn integrator using the internal generator BPACKT (degrees per sidereal day)

$\dot{\lambda}_i$ = base drift rate as calculated in Equation (2-22) (degrees per sidereal day)

$\dot{\lambda}_{ii}$ = drift rate obtained by propagating the Keplerian osculating elements from the user-specified orbit source at ignition time using the internal generator BPACKT (degrees per sidereal day)

The term $(\dot{\lambda}_i - \dot{\lambda}_{ii})$ combines into one term the mismodeling of the internal generator (BPACKT). Included in this term are all orbit perturbations not modeled in BPACKT (e.g., the effects of the Sun and the Moon on the drift rate). Another way of interpreting Equation (2-24) is to assume that $\dot{\lambda}_i$ fixes the drift rate at ignition time and that any change in the semimajor axis will cause a corresponding change in the drift rate. $\dot{\lambda}_T - \dot{\lambda}_{ii}$ is the expression for the change in the drift rate resulting from a change in the semimajor axis. For small burns ($\leq$ 500 seconds), the mismodeling error $(\dot{\lambda}_i - \dot{\lambda}_{ii})$ will remain relatively constant. For burns of the hydrazine thrusters aboard ATS-6 longer than 500 seconds, the mismodeling error becomes relatively insignificant compared to the desired change in drift rate. If the effects of the Sun and the Moon were modeled in the internal generator BPACKT, the mismodeling error would approach zero and the two methods of computing the drift rate (before and during thrusting) would be equivalent.

2.3.1.2 Iteration Scheme for Drift Rate Maneuvers

As stated earlier, CNTRLF is designed on the principle of obtaining an estimate of the burn time and then modeling the burn to verify that this estimate will produce the desired maneuver goals. If the estimate does not produce the specified goals, an iteration scheme is applied to refine the estimate. For drift rate changes while thrusting in the reference attitude orientation, the maneuver can start at any time and the maneuver goal can always be achieved. In other words, although the maneuver may not be executed at the most fuel efficient time (i.e., at a apsis), the maneuver goal will be met. When thrusting in the other possible attitude modes, however, there will be positions in the orbit where the maneuver goal cannot be met. No attempt is made in CNTRLF to refine the user-specified ignition time. Rather, the ignition time is held at its user-specified value, while the burn time is adjusted to meet the specified maneuver objectives. If the input attitude configuration is such that the thruster is not aligned with the velocity vector, a fuel optimum solution will not be found. In this case a warning message is printed to alert the user, but the computation proceeds. The burn time is updated at each iteration step as follows:

1. The drift rate algorithm (Section 2.3.1.1) is used to obtain a drift rate at the end of a burn.

2. The semimajor axis corresponding to the drift rate after the burn is calculated using Equation (2-14).

3. This semimajor axis is subtracted from the desired semimajor axis--also calculated by Equation (2-14)---to obtain an error term. The error term represents the magnitude of the error in the estimated burn time.

4. Using Equation (2-21), this error in the semimajor axis is converted into an error in ΔV .

5. The error in ΔV is then converted to an error in burn time by using the rocket equation:

$$\Delta T = W_f \frac{e^{(\Delta\Delta V/(G\ ISP))} - 1}{\dot{W}} \qquad (2\text{-}25)$$

where ΔT = the error time increment used to update the previous estimate of burn time (seconds)

W_f = the expected fuel weight at the end of the maneuver pounds

$\Delta\Delta V$ = the error in ΔV between the maneuver goal achieved and the desired maneuver goal (calculated in previous step) (feet per second)

G = gravitational acceleration constant at Earth's surface (32.174 feet per second^2)

ISP = specific impulse of engine to be used (the expected ISP at the end of the burn) (seconds)

$\dot{W}$ = rate of fuel usage for the engine to be used (pounds per second) i.e., $\dot{W} = T/ISP$ where T equals the thrust of the engine to be used (pounds) (the expected thrust at the end of the burn)

2.3.2 Derivation of ΔV Magnitude For Inclination/Node Change Maneuvers

Inclination or node maneuvers (plane change maneuvers) take place at the intersection of the plane of the initial orbit and the plane of the final orbit (line of relative nodes). The initial orbit plane expressed in osculating Keplerian elements is obtained from the orbit source selected by the user. In general, the orbital vector read from the source will be at a time specified by the user. This time will not be the ignition time, as in the drift rate scheme (Section 2.3.1.2), but will be an arbitrary time normally chosen very close to the desired maneuver time. The CNTRLF program will calculate an ignition time which will be as close to this arbitrary time as possible ($\pm$ one orbit period) and permit the north-south maneuver goals to be met. The final orbit

plane is also expressed in osculating Keplerian elements defined by the maneuver goals specified by the user. A change in the orbit plane due to thrusting can be represented by the following Lagrange equations (see Reference 1):

$$\frac{d\Omega}{dt} = \frac{r \sin u}{na^2\sqrt{1 - e^2}\sin i} W \tag{2-26}$$

and

$$\frac{di}{dt} = \frac{r \cos u}{na^2\sqrt{1 - e^2}} W \tag{2-27}$$

where

u = argument of latitude (argument of perigee plus true anomaly) of maneuver point (radians)

r = magnitude of orbit radius vector (ERU)

a = semimajor axis (ERU)

n = mean motion (radians per second)

e = eccentricity (dimensionless)

W = orbit normal acceleration (ERU per second^2)

di, $d\Omega$, dt = differentials of inclination, node, and time, respectively

The Lagrange Equations (2-26) and (2-27) can be modified by replacing Wdt by dV (velocity differential) and by setting $na^2\sqrt{1 - e^2}/r$ equal to V_0 (orbital velocity). The modifications result in the following equations:

$$d\Omega = \frac{\sin u}{V_0 \sin i} dV \tag{2-28}$$

$$di = \frac{\cos u}{V_0} dV \tag{2-29}$$

Taking the partial derivatives of the changes in the node and the inclination with respect to the argument of latitude results in

$$\frac{\partial(d\Omega)}{\partial u} = \frac{\cos u}{V_0 \sin i}\, dV \tag{2-30}$$

$$\frac{\partial(di)}{\partial u} = \frac{-\sin u}{V_0}\, dV \tag{2-31}$$

Taking the partial derivatives of the changes in the node and the inclination with respect to the dV results in

$$\frac{\partial(d\Omega)}{\partial(dV)} = \frac{\sin u}{V_0 \sin i} \tag{2-32}$$

$$\frac{\partial(di)}{\partial(dV)} = \frac{\cos u}{V_0} \tag{2-33}$$

By expanding the above results into a series,

$$d(d\Omega) = \frac{\cos u\, dV}{V_0 \sin i}\, du + \frac{\sin u}{V_0 \sin i}\, d(dV) \tag{2-34}$$

$$d(di) = \frac{-\sin u\, dV}{V_0}\, du + \frac{\cos u}{V_0}\, d(dV) \tag{2-35}$$

Solving Equations (2-34) and (2-35) simultaneously, using Cramer's rule results in

$$du = \frac{V_0}{dV} [d(d\Omega) \sin i \cos u - d(di) \sin u] \tag{2-36}$$

$$d(dV) = V_0 [d(d\Omega) \sin i \sin u + d(di) \cos u] \tag{2-37}$$

Approximate solutions of Equations (2-36) and (2-37) can be obtained if the finite differences are assumed to be equivalent to the differentials of these equations. The finite differences of Equations (2-36) and (2-37) take the forms

$$\Delta u = \frac{V_0}{\Delta V} \{ [\Delta\Delta \Omega \sin i_{av} \cos u] - (\Delta\Delta i \sin u) \} \tag{2-38}$$

$$\Delta\Delta V = V_0 \{ [\Delta\Delta \Omega \sin i_{av} \sin u] + (\Delta\Delta i \cos u) \} \tag{2-39}$$

where Δu = the finite change in the argument of latitude (radians)

$\Delta\Delta V$ = the finite change in the change in velocity increment (feet per second)

$\Delta\Delta\Omega$ = the finite change in the change in node (radians)

$\Delta\Delta i$ = the finite change in the change in inclination (radians)

i_{av} = the average inclination ($\Delta i/2$) (radians)

V_c = orbital velocity

u = argument of latitude

2.3.2.1 Calculation of the Time of Relative Nodes

Solving Equations (2-28) and (2-29) simultaneously results in the following expression for argument of latitude:

$$u = \arctan\left(\frac{\sin i \, d\Omega}{di}\right) \tag{2-40}$$

where u = argument of latitude (argument of perigee plus true anomaly) (radians)

i = inclination (radians)

di, $d\Omega$ = differentials of inclination and node

Taking finite differences,

$$u = \arctan\left(\frac{\sin i_{av} \, \Delta\Omega}{\Delta i}\right) \tag{2-41}$$

From the argument of latitude, the eccentric anomaly can be found

$$f = u - \omega \tag{2-42}$$

where f = true anomaly (radians)

u = argument of latitude (radians)

ω = argument of perigee (radians)

Then, from Reference 6

$$ECC = 2 \arctan\left[\sqrt{\frac{1 - e}{1 + e}} \tan\left(\frac{f}{2}\right)\right] \tag{2-43}$$

where ECC = eccentric anomaly (radians)

e = eccentricity (dimensionless)

The mean anomaly corresponding to the time of relative nodes is found from the eccentric anomaly.

$$m = ECC - e \sin (ECC) \qquad (2\text{-}44)$$

where m = mean anomaly (radians)

By subtracting this mean anomaly from the current mean anomaly and dividing by the mean motion of the orbit, the time from the current time to the relative node is found. If the computed time is before the epoch of the orbit source, it is moved forward as many orbital periods necessary to place the time of relative nodes after epoch.

2.3.2.2 Calculation of First Estimate of Burn Time and Ignition Time

Knowing the time of relative nodes and an initial estimate of ΔV, the first estimates of the burn time and the ignition time can be calculated. The first estimate of the burn time is calculated using Equation (2-25). The values of ISP and the fuel expenditure rate $\dot{W}$ are obtained at the start of the burn rather than at the end. Also the initial estimate of ΔV is used in place of $\Delta\Delta V$. The estimated burn time is centered about the line of relative nodes to obtain a first estimate of the ignition time.

2.3.2.3 Integration Scheme for Inclination/Node Maneuvers

An integration scheme is used with the inclination/node maneuvers to converge on a burn time (as with the drift rate change maneuvers) and an ignition time which will meet the user-specified maneuver goals. At each stage of the iteration, the burn time and the ignition time are updated according to the following procedure:

1. An error is developed between the calculated final orbital inclination/node and the desired inclination/node.

2. The errors in inclination and node become the $\Delta\Delta i$ and $\Delta\Delta\Omega$, respectively, in Equations (2-38) and (2-39).

3. Equation (2-39) is solved for $\Delta\Delta V$. The $\Delta\Delta V$ is converted to an error in burn time using the Equation (2-25).

4. Equation (2-38) is solved for Δu. The Δu is converted to an error in ignition time by dividing the results by the mean motion (n) of the orbit.

2.3.3 Stationkeeping

Section 2.3.1 described the derivation of ΔV for drift rate change maneuvers. It was stated that the goal drift rate and the ignition time would be either user-specified or, in the case of east-west stationkeeping, calculated by CNTRLF. This section describes the calculation of the drift rate goal and the ignition time for east-west stationkeeping maneuvers. Section 2.3.3.1 discusses the stationkeeping strategy incorporated in CNTRLF and Section 2.3.3.2 describes the specific targeting algorithm used.

2.3.3.1 Stationkeeping Strategy

The perturbing forces on an artificial statellite in orbit about the Earth are:

1. The Earth's gravitational field
2. The gravitational attractions of the Sun, the Moon, and the planets
3. The Earth's atmosphere
4. The Earth's magnetic field
5. Solar radiation

For circular, equatorial, synchronous orbits (well outside of the Earth's atmosphere), the Earth's gravitational field and the gravitational attraction of the Sun and the Moon are the major perturbing forces. If it is assumed that the Earth is symmetrical about its polar axis, the magnitude of the Earth's potential field should be solely a function of the distance from the center of mass.

In general, the Earth's potential field departs slightly from that of a body having axial symmetry. The potential field varies not only as a function of distance from the Earth's center, but also as a function of longitude. The accelerated drift introduced in 24-hour orbits, due to the Earth's anomalous potential, is described mathematically in Reference 9 as:

$$\ddot{\lambda} = 12\pi^2 \sum_{\substack{\ell-m \\ \text{even}}} C_{\ell m} [F_{\ell m} \sin m\lambda] + S_{\ell m}[-F_{\ell m} \cos m\lambda] \qquad (2\text{-}45)$$

where $\ddot{\lambda}$ = rate of change of drift rate (acceleration) due to the Earth not having axial symmetry (degrees per sidereal day^2)

λ = subsatellite longitude (degrees east)

$C_{\ell m}$, $S_{\ell m}$ = harmonic coefficients of the Earth's potential field

$F_{\ell m}$ = term to correct for inclination:

$$F_{22} = \frac{6}{a^2}\left[\frac{1}{2}(1 + \cos i)\right]^2$$

$$F_{31} = \left(\frac{-3}{2a^3}\right)\left[\frac{1}{2}(1 + \cos i) + \frac{5}{8}\sin^2 i\,(1 + 3\cos i)\right]$$

$$F_{33} = \left(\frac{45}{a^3}\right)\left[\frac{1}{2}(1 + \cos i)\right]^3$$

$$F_{42} = \left(\frac{-15}{a^4}\right)\left[\frac{1}{4}(1 + \cos i)^2 - \frac{7}{4}\sin^2 i \cos i\,(1 + \cos i)\right]$$

$$F_{44} = \left(\frac{420}{a^4}\right)\left[\frac{1}{2}(1 + \cos i)\right]^4$$

a = semimajor axis (ERU)

i = inclination (radians)

Included are the even ℓ-m terms up to the higher order $\ell = 4$, $m = 4$ term. The constants $C_{\ell m}$ and $S_{\ell m}$ are measures of the amplitudes of the various spherical harmonic coefficients of the Earth's potential field. These terms are referred to as tesseral harmonic coefficients. Values for these terms have been derived by examining the orbits of high altitude satellites. The following values used by the Goddard Trajectory Determination System (GTDS) are also used in CNTRLF (Reference 10):

ℓ	m	C	S
2	2	$.1566511 \times 10^{-5}$	$-.8969932 \times 10^{-6}$
3	1	$.2161875 \times 10^{-5}$	$.2571596 \times 10^{-6}$
3	3	$.1025055 \times 10^{-6}$	$.1949036 \times 10^{-6}$
4	2	$.7739965 \times 10^{-7}$	$.1515418 \times 10^{-6}$
4	4	$-.3608512 \times 10^{-8}$	$.6386659 \times 10^{-8}$

Due to the tesseral acceleration, a synchronous satellite placed in an equatorial orbit over a specified subsatellite point will drift slowly from its assigned station. If left to drift, the satellite would drift toward a station on the Earth's minor axis (see Figure 2-7). Like a pendulum, it would then reasonate about this axis. For this reason, active stationkeeping strategy is needed to maintain the satellite position within some specified constraints.

A scheme which has been used successfully with other operational synchronous satellites is to choose two boundaries, one on either side of a nominal station longitude, and to keep the spacecraft within these boundaries by exercising active thruster control. Figure 2-8 illustrates the sequence of events in normal east-west stationkeeping. The satellite drifts slowly until it reaches the boundary that is between the normal station longitude and the closest minor axis. At this point, a maneuver must be performed, or the satellite will drift

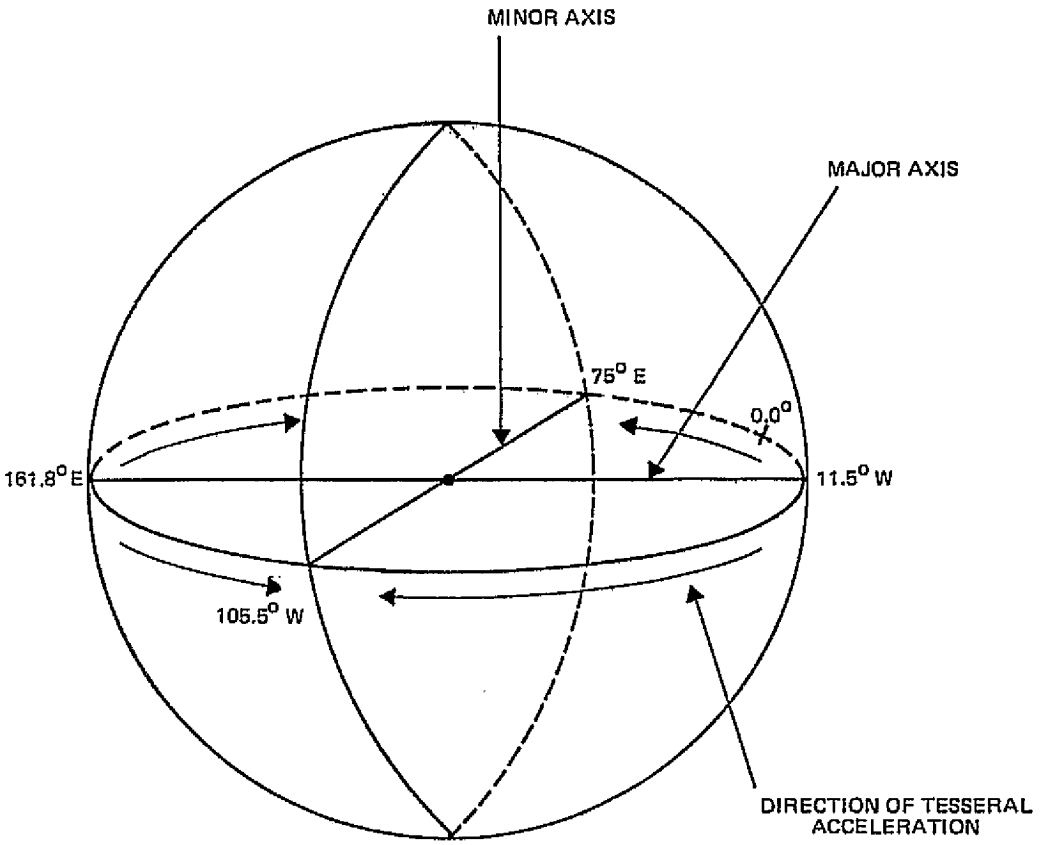

Figure 2-7. Earth Model Not Symmetric About Its Polar Axis

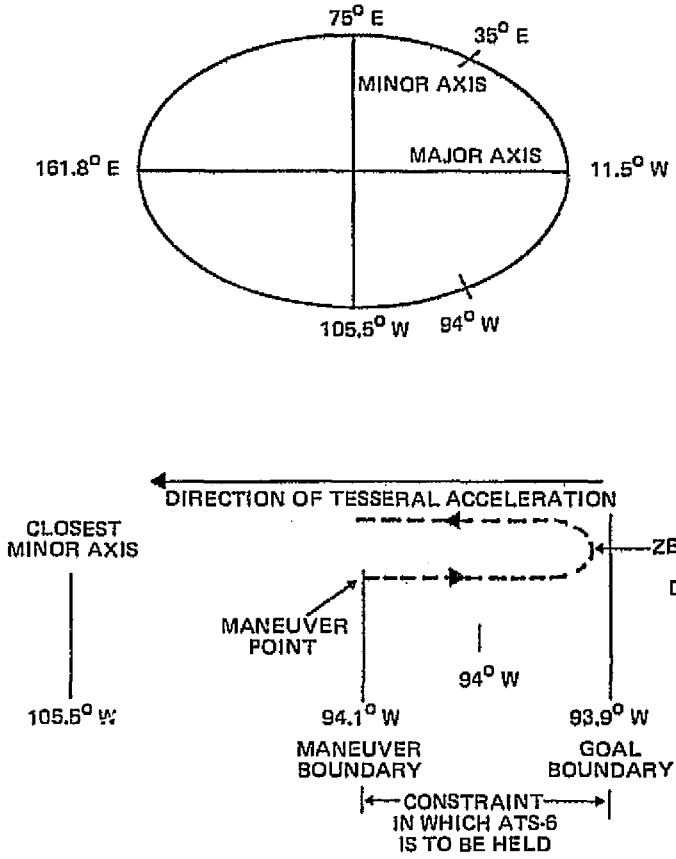

Figure 2-8. ATS-F Stationkeeping At Two Stations

outside of the boundary. The calculated maneuver gives the satellite the desired drift rate in the opposite direction, i.e., toward the second boundary. The required impulse is calculated so that the effect of the tesseral acceleration reduces the drift rate to zero when the satellite reaches the second boundary. The continued action of the tesseral forces then starts the satellite back toward the maneuver boundary. When the first boundary has been again reached, another stationkeeping maneuver is performed, and the cycle is repeated. Typically, this drift cycle (time between stationkeeping maneuvers) is from 30 days to 80 days. In the scheme described above, calculation of the required impulse in CNTRLF is based on Equation (2-45) (perturbations due to tesseral acceleration only). However, as stated earlier, the gravitational attraction of the Sun and the Moon are also major perturbing forces. Because the impulse calculated by CNTRLF is correct only in the absence of a solar and a lunar gravitational field, the maneuvers calculated will result in minor overshoots or undershoots of the goal boundary.

2.3.3.2 Targeting Algorithm

In CNTRLF, a user can specify an east-west stationkeeping maneuver in two ways. In the first method, two average subsatellite longitude boundaries as well as a search start time, stop time, and time increment are input to CNTRLF. The program searches the specified orbit source until either of the two longitudes is crossed by the satellite or until the search stop time is reached. If a boundary crossing occurs, a maneuver is then calculated. If no boundary is crossed, an error message is printed and CNTRLF exits. In the second method, the input consists of the time that the maneuver is to be performed and one longitude boundary. The input longitude boundary and the average longitude at the input time define the boundaries in which the satellite is to be constrained (see Figure 2-8). The average longitude calculated at the input time serves as the maneuver boundary, while the input longitude defines the goal boundary. With the time of the maneuver now known (either the result of a

search or entered directly, a goal drift rate is determined. Based on the concepts developed in Section 2.3.3.1, the following algorithm is used to calculate a goal drift rate

1. Determine within which quadrant the maneuver falls

Quadrant	Boundaries
IQUAD(1)	11.5 degrees west - 75 degrees east
IQUAD(2)	75 degrees east - 161.8 degrees east
IQUAD(3)	161.8 degrees east - 105.5 degrees west
IQUAD(4)	105.5 degrees west - 11.5 degrees west

2. If within quadrant 1 or 3, the calculation will result in either a zero or a positive drift rate

3. If within quadrant 2 or 4, the calculation will result in either a zero or a negative drift rate

4. If the maneuver boundary is closer to the minor axis than the goal boundary, the drift rate goal is calculated as follows:

$$\dot{\lambda} = \pm \sqrt{2 \ddot{\lambda} \Delta\lambda} \qquad (2\text{-}46)$$

where $\dot{\lambda}$ = calculated drift rate (degrees per day); sign determined by quadrant in which satellite lies

$\ddot{\lambda}$ = tesseral acceleration calculated using Equation (2-45); longitude used in Equation (2-45) is that of the desired desired station--center of the tolerance box (degrees per day^2)

$\Delta\lambda$ = distance between the two longitudinal constraints (degrees)

5. If the maneuver boundary is farther from the minor axis than the goal boundary, the drift rate goal is zero.

2.4 HYDRAZINE ENGINE PROPULSION MODEL

The hydrazine engine propulsion model includes the models for the following procedures:

1. For a time segment of Δt seconds (continuous firing mode), computing the weight of fuel expended and update the tank pressure and spacecraft weight as a result of this fuel expenditure.
2. For a time segment of Δt seconds, computing the effective impulse and ΔV delivered by the control jet
3. Interpolating the control jet calibration tables as necessary

2.4.1 Fuel Weight Expenditure

The hydrazine propulsion model used in CNTRLF computes the weight ΔW of fuel expended during Δt seconds of continuous firing.

$$\Delta W = \frac{1}{2}(\dot{W}_{i+1} + \dot{W}_i)\Delta t \qquad (2\text{-}47)$$

where ΔW = the weight of fuel expended during Δt seconds of continuous firing (pounds)

$\dot{W}_{i+1}$ = rate of fuel expenditure at the end of Δt time segment; obtained by interpolating the $\dot{W}$ calibration tables (pounds per second)

$\dot{W}_i$ = rate of fuel expenditure at the start of the Δt time segment; obtained by interpolating the $\dot{W}$ calibration tables (pounds per second)

The problem of computing ΔW reduces to interpolating the $\dot{W}$ calibration tables. These tables (see Section 2.4.3) express $\dot{W}$ as a function of engine type, pressure, and time. The engine type and time are known. The pressure selected for the interpolation will be the average pressure P_{av} between the initial pressure P_i at the start of the time segment and the final pressure P_f at the end of the time segment.

$$P_{av} = \frac{P_0 + P_f}{2} \tag{2-48}$$

where P_{av} = average pressure in time segment (pounds per square inch absolute (PSIA))

P_0 = initial pressure at start of the time segment (PSIA)

P_f = final pressure at the end of the time segment (PSIA)

The pressure at the beginning of the time segment is known. Using Boyle's law, the pressure at the end of the time segment, P_f, is expressed as follows:

$$P_f = \frac{PCON}{W_0^* + \Delta W} \tag{2-49}$$

where P_f = final pressure at the end of the time segment (PSIA)

PCON = pressure-volume constant of the fuel pressurant given by

$$PCON = P_I \left(WFULL - W_{fuel_I} \right)$$

P_I = tank pressure at the start of the maneuver---not of the time segment (PSIA); input to CNTRLF program

WFULL = weight of fuel required to fill the tank completely (pounds); data in spacecraft calibration data base (see Section 2.4.3)

W_{fuel_I} = weight of fuel at start of the maneuver (pounds); input to CNTRLF program

W_0^* = relative pressurant volume at the start of a time segment (pounds) given by

$$W_0^* = WFULL - W_{fuel_0}$$

(volume is proportional to weight)

W_{fuel_0} = weight of fuel at the start of a time segment (pounds); internal variable maintained by CNTRLF

ΔW = weight of fuel expended (pounds)

Equation (2-49) reflects the decrease in tank pressure due to the expanding volume of pressurant as fuel is depleted from the tank.

To calculate the fuel expended in a time segment, Equation (2-47) indicates that the rate of fuel expenditure curves must be interpolated. To interpolate, the average pressure P_{av} during the time segment must be ' -n. P_{av} is a function of the final pressure which is a function of the weigt expended. In CNTRLF, ΔW is determined iteratively using Equations (2-47), (2-48), and (2-49) as follows:

1. An initial estimate of ΔW is made: $\Delta W = 0.0$; thus, $P_f = P_i$ and $P_{av} = P_i$.

2. Using Equation (2-47), ΔW is solved using $P_{av} = P_i$ to interpolate the $\dot{W}$ calibration tables. The interpolated $\dot{W}$ value is corrected for individual jet performance by multiplying the value by a user-specified calibration factor.

3. A comparison is made between the ΔW estimated and the ΔW calculated. If the difference is less than 0.00001 pound, the correct ΔW and P_{av} have been found.

4. If ΔW estimated and ΔW calculated differ by more than 0.00001 pound, use as a new estimate of ΔW the previously calculated value. This value of ΔW is used in Equation (2-49) to determine a new value for the final pressure at the end of the time step P_f. All values in Equation (2-49) are known at the start of the time step except $\Delta\dot{W}$. Now, solve Equation (2-48) for a new estimate of P_{av}.

5. Next, Equation (2-47) is solved for ΔW using the P_{av} value calculated using Equation (2-48) to interpolate the $\dot{W}$ calibration tables. The interpolated $\dot{W}$ value is corrected for individual jet

performance by multiplying the value by a user-specified calibration factor.

6. Step 4 in which a comparison is made between the estimated ΔW and the calculated ΔW is repeated.

In the above iteration, both the fuel expended in a Δt time segment and the average pressure P_{av} during that time segment are calculated. If after 20 iterations the estimated ΔW and computed ΔW differ by greater than 0.00001 pound, an error message is printed and the final calculated value of ΔW is used.

2.4.2 Effective Impulse and ΔV

Once the fuel expended and the average pressure during a Δt time segment have been determined, the following calculations are made:

$$EFFIMP = \frac{N \cos \alpha_c}{2} (T_1 + T_2) \Delta t \qquad (2\text{-}50)$$

where EFFIMP = effective impulse (pound/seconds)

N = number of thrusters used:
= 1, if an east-west stationkeeping maneuver is performed
= 2, if a north-south maneuver is performed

α_c = cant angle which introduces a radial component of thrust for both eastward and westward thrusting; for north-south maneuvers the cant angle is set to zero degree

T_1 = thrust at the beginning of the ΔT time increment (pounds)

T_2 = thrust at end of ΔT time increment (pounds)

Δt = time segment in which calculation is to be made; generally lies between 1 second and 100 seconds

T_1 and T_2 are found by interpolating the thrust calibration table (see Section 2.4.3) at the beginning and end of the Δt time increment and with pressure

equal to the average pressure during the time step P_{av}. The interpolated thrust is corrected for individual jet performance by multiplying the value by a user-specified calibration factor.

$$AVEISP = EFFIMP/\Delta W \tag{2-51}$$

where AVEISP = average ISP over time interval Δt

EFFIMP = effective impulse from Equation (2-50)

ΔW = fuel expended during Δt time segment; calculated iteratively (see Section 2.4.1)

$$DELVL = AVEISP\ G \left(\log \frac{W_0}{W_F} \right) \tag{2-52}$$

where DELVL = ΔV expended due to thrusting during Δt time segment (feet per second)

G = acceleration of gravity at Earth's surface (32.174 feet per second^2)

W_0 = spacecraft's weight before incremental burn; the weight at the start of the burn is put into CNTRLF; the spacecraft's weight is recalculated after each Δt time segment (pounds)

W_F = spacecraft's weight after incremental burn (pounds); calculated by the expression $W_F = W_0 - \Delta W$; used as W_0 value in the next time segment

2.4.3 Thruster Model Data Base

The jet calibration tables are stored internally in CNTRLF. The data is in tabular form and consists of the best available thruster data from ground tests (see Appendix A). The following list describes the data required by the engine models of CNTRLF.

Symbol	Definition	Units
G	Gravitational constant on Earth's surface	Feet per second squared
α	Hydrazine engine cant angle	Radians
THRION	Thrust of ion engine	Pounds
XISP	ISP of ion engine	Seconds
N	Number of hydrazine engines modeled; a maximum of two are allowed. CNTRLF presently uses one model with the individual thrusters varying from the model by a user-specified calibration factor	Not applicable
NOTMPS	Number of tank temperatures at which hydrazine thruster data is available; FDATA uses at least three temperature curves	Not applicable
TABTMP	Inlet temperatures at which thruster data is available	Degrees Fahrenheit
TABVOL	Array of weights of fuel in tanks when completely full (WFULL). There is one value for each inlet temperature	Pounds
NOPRES[1]	Number of pressure data points on individual temperature curves	Not applicable
TABPRS	Pressures corresponding to points on temperature curves	Pounds per square inch
NOTIME[1]	Number of time data points on individual temperature curves	Not applicable
TABTIM	Time corresponding to points on temperature curve	Seconds
TABISP	A four-dimensional array representing specific impulse at a specified time, pressure, and inlet temperature for a specific engine model	Seconds

[1]The number of time points and pressure points must be the same for each inlet temperature curve. The values of time and pressure at these points can be different.

Symbol	Definition	Units
TABF	A four-dimensional array representing thrust at a specified time, pressure, and inlet temperature for a specific engine model	Pounds
TSEG	Maximum burn time of a hydrazine thruster	Minutes
DELSEG	Minimum allowable time between successive actuations of the hydrazine thrusters	Minutes

As new data becomes available, an internal subroutine (FDATA) will be modified and recompiled. Currently, ATS-6 flight test data are incorporated in the program. The current data and format are shown in Figure 2-9.

Based on an input tank temperature, the data in TABVOL are interpolated (see Equation (2-54)) to obtain a current value for the amount of fuel required to completely fill the tanks (WFULL). Based on an input tank temperature, the data in TABISP and TABF are interpolated (see Equation (2-54)) to obtain data describing ISP and thrust at that temperature. The thrust data is divided by the ISP data on a point-by-point basis to obtain data on the rate of fuel expenditure.

$$\dot{W} = \frac{T}{ISP} \tag{2-53}$$

where $\dot{W}$ = rate of fuel expenditure at a specified time and pressure (pounds per second)

T = thrust at the same time and pressure (pounds)

ISP = ISP at the same time and pressure (seconds)

All data points are indexed by type of jet modeled, time, and pressure. The fuel expenditure rate data $\dot{W}$ and the thrust data T are used in the calculation of fuel expended ΔW and average pressure P_{av} during an incremental time step Δt (see Section 2.4.1). Specific values for $\dot{W}$ and T at a given time and pressure are found by interpolation. A linear interpolation scheme is used

```
C
C  ***ATS-F CONSTANTS
C
      GG=32.174D0
      ALPH=0.297302D0
      THRICN=0.0D0
      XISP=2500.0D0
C
C  ***ENGINES AVALIABLE
C
      NOENGS=1
C
C  ***TEMP (DEG F.)              TABTMP(NOTMPS,NOENGS)
C
      NOTMPS=3
      REAL*8 TABTMP(3,1)        /41.000,
     *                           70.000,
     *                           95.000/
C
C  *** WEIGHT OF FUEL IN EMPTY TANK
C      A VALUE FOR EACH TEMPERATURE REQUIRED
C
      REAL*8 TABVOL(3,1)        /85.35400,
     *                           84.09400,
     *                           83.16000/
C
C  ***PRES (PSI.)                TABPRS(NOPRES,NOTMPS,NOENGS)
C
      NOPRES=2
      REAL*8 TABPRS(2,3,1)      /150.000,350.000,
     *                           150.000,350.000,
     *                           150.000,350.000/
C
C  ***TIME (SEC.)                TABTIM(NOTIME,NOTMPS,NOENGS)
C
      NOTIME=3
      REAL*8 TABTIM(3,3,1)      /0.000,1.000,20000.000,
     *                           0.000,1.000,20000.000,
     *                           0.000,1.000,20000.000/
C
C  ***ISP ARRAY (SEC.)           TABISP(NOTIME,NOPRES,NOTMPS,NOENGS)
C
      REAL*8 TABISP(3,2,3,1) /213.100,213.100,213.100,
     *                        222.100,222.100,222.100,
     *                        213.100,213.100,213.100,
     *                        222.100,222.100,222.100,
     *                        213.100,213.100,213.100,
     *                        222.100,222.100,222.100/
C
C  ***THRUST ARRAY (LBS.)        TABF  (NOTIME,NOPPES,NOTMPS,NOENGS)
C
      REAL*8 TABF   (3,2,3,1) /0.000,0.057500,0.057500,
     *                         0.000,0.118400,0.118400,
     *                         0.000,0.057500,0.057500,
     *                         0.000,0.118400,0.118400,
     *                         0.000,0.057500,0.057500,
     *                         0.000,0.118400,0.118400/
C
C  ***INITALIZE BURN TIME INTERUPTS
C
C     ATS-F NO INTERUPTS DUE TO TIME ENGINE FIRES
C
C           TSEG WHICH IS THE TIME ENGINE CAN FIRE CONTINUOUSLY
C                BEFORE AN INTERUPT WILL OCCURE IS MAX (720 MIN.)
C        DELSEG WHICH IS THE DELAY BEFORE ENGINE CAN BE FIRED
C                AGAIN IS ZERO (0.0 MIN.)
C
      TSEG=720.0D0
      DELSEG=0.0D0
C
C  ****
C  ***END OF DATA
C  ****
C
```

Figure 2-9. Current ATS-6 Thruster Data at Three Temperatures

(see Equation (2-54)) unless the current pressure falls within the three lowest pressure points; if this happens, a quadratic interpolation method is used. The data are interpolated first with respect to pressure and then time using the following equation:

$$F_X = F_{XL} + \left(F_{XU} - F_{XL}\right)\theta \tag{2-54}$$

$$\theta = \frac{X - X_L}{X_U - X_L} \tag{2-55}$$

where X = independent variable

X_L = lower independent variable data point

X_U = upper independent variable data point

F_{XL} = lower dependent variable data point

F_{XU} = upper dependent variable data point

F_X = interpolated answer

In the above scheme, the independent variables are pressure and time, while the fuel expenditure rate and the thrust are dependent variables.

Included in the list of data required by the CNTRLF engine models are the ion engine parameters. These parameters are constant and do not vary as a function of time and pressure as do the hydrazine engine parameters.

2.5 FINITE BURN INTEGRATION MODEL

Once the amount of fuel expended and ΔV magnitude produced during an incremental burn are calculated, then the changes in the orbital elements due to the thrusting of a hydrazine engine are calculated. To calculate these changes requires knowledge only of the inertial position and velocity vectors at the start of the burn segment and of the type of engine being used. The Earth is

treated as a point source and a standard numerical technique is used to integrate the $\ddot{\vec{R}}$ equation, which is

$$\ddot{\vec{R}}_f = -\mu \frac{\vec{R}}{R^3} + \Delta\Delta V \, \hat{T} \qquad (2\text{-}56)$$

where $\ddot{\vec{R}}_f$ = final acceleration vector (ERU per second^2)

μ = gravitational attraction constant of the Earth (32.174 feet per second^2)

$\vec{R}$ = calculated position vector representing the spacecraft position at the end of a calculation time step (ERU); at ignition time, this value is obtained from the user-specified orbit source

$\Delta\Delta V$ = rate of change of ΔV during the incremental time step (feet per second)

$\hat{T}$ = thrust direction unit vector in inertial coordinates; calculated each ΔT time step using the transformation described in in Section 2.2

The specific numerical technique used in the fourth-order Adams-Moulton predictor-corrector integration scheme. To start the predictor-corrector, a modified second-order Runge-Kutta method is used. In this method, the following equations, which are integrals of the $\ddot{\vec{R}}$ equation, are solved:

$$\vec{V}_f = \vec{V}_i - \frac{\mu \vec{R}_{ave}}{R^3} \Delta T + \Delta V \hat{T}_{ave} \qquad (2\text{-}57)$$

$$\vec{R}_f = \vec{R}_i + \vec{V}_{ave} \Delta T + DVR \; \hat{T}_{ave} \Delta T \qquad (2\text{-}58)$$

where $\vec{V}_f$ = velocity vector of the spacecraft at the end of the time step (ERU per second)

$\vec{R}_f$ = position vector of the spacecraft at the end of the time step (ERU)

$\vec{V}_{ave}$ = estimated velocity vector[1] in the middle of the time step (ERU per second)

$\vec{R}_{ave}$ = estimated position vector[1] in the middle of the time step (ERU)

$\hat{T}_{ave}$ = estimated thrust direction vector[1] in the middle of the time step (unit vector)

$\vec{V}_i$ = initial velocity vector at the beginning of the time step (ERU per second)

$\vec{R}_i$ = intial position vector at the beginning of the time step (ERU)

Δt = incremental time step (seconds)

ΔV = change in orbital velocity due to thrusting calculated using Equation (2-52) (ERU per second)

DVR = integral of ΔV defined by the following equation (with all variables defined as in Section 2.4.2)

$$DVR = AVEISP\ G\left[\frac{W_F}{\Delta W}\ \ell n\left(\frac{W_0}{W_F}\right) - 1\right] \qquad (2\text{-}59)$$

The starter method is used only for three Δt time intervals before the Adams-Moulton method of numerical integration is initiated. If the Δt time interval changes (e.g., at the end of the maneuver), the Adams-Moulton method is restarted with the modified second-order Runge-Kutta.

[1]The estimated velocity, position, and thrust directions are calculated by advancing the mean anomaly of the osculating elements at the end of the previous time step by half a time step, then converting the resulting osculating elements into inertial elements.

The fourth-order Adams-Moulton predictor-corrector is defined mathematically as follows:

Adams-Moulton predictor:

$$\vec{PV} = \vec{V}_i + \frac{\Delta T}{24}(55\vec{A}_i - 59\vec{A}_{i-1} + 37\vec{A}_{i-2} - 9\vec{A}_{i-3})$$
$$\vec{PR} = \vec{R}_i + \frac{\Delta T}{24}(55\vec{V}_i - 59\vec{V}_{i-1} + 37\vec{V}_{i-2} - 9\vec{V}_{i-3}) \qquad (2\text{-}60)$$

Adams-Moulton corrector:

$$\vec{CV} = \vec{V}_i + \frac{\Delta T}{24}(9\vec{PA} + 19\vec{A}_i - 5\vec{A}_{i-1} + \vec{A}_{i-2})$$
$$\vec{CR} = \vec{R}_i + \frac{\Delta T}{24}(9\vec{PV} + 19\vec{V}_i - 5\vec{V}_{i-1} + \vec{V}_{i-2}) \qquad (2\text{-}61)$$

where $\vec{PA}$ = predicted acceleration calculated using the $\ddot{R}$ Equation (2-56) (ERU per second^2)

$\vec{PV}$, $\vec{PR}$ = predicted velocity and position vectors[1] of the spacecraft at the end of the incremental time step (ERU per second)

$\vec{CV}$, $\vec{CR}$ = corrected velocity and position vectors[1] at the end of the incremental time step (ERU per second)

$\vec{A}_i$, $\vec{V}_i$, $\vec{R}_i$ = acceleration, velocity, and position vectors of the spacecraft at the beginning of the time step

$\vec{A}_{i-x}$, $\vec{V}_{i-x}$ = acceleration and velocity vectors of the spacecraft at either one, two, or three time steps previous to the beginning of the current time step

[1] The predicted R and calculated R should not differ by more than a tolerance of 1×10^{-9} ERU . If they do an iteration scheme is entered until they converge within this tolerance.

CNTRLF maintains both an acceleration and velocity array where the following substitutions take place at the end of every time step:

$$\vec{A}_{i-3} = \vec{A}_{i-2}$$

$$\vec{V}_{i-3} = \vec{V}_{i-2}$$

$$\vec{A}_{i-2} = \vec{A}_{i-1}$$

$$\vec{V}_{i-2} = \vec{V}_{i-1}$$

$$\vec{A}_{i-1} = \vec{A}_{i}$$

$$\vec{V}_{i-1} = \vec{V}_{i}$$

The final position and velocity vectors are transformed into Keplerian osculating elements using the method discussed in Section 2.1.5.

2.6 ION ENGINE THRUST PERTURBATION MODEL

Sections 2.4 and 2.5 describe the effects of thrusting the hydrazine engines for an incremental time step. The following section describes the effects of thrusting the Cesium bombardment engine for an incremental time step.

The thrust level of the ion engines onboard ATS-6 is on the order of 0.001 pound force, and the specific impulse is about twenty-five hundred seconds. The thrust does not vary as a function of time or pressure and is only slightly greater (by a factor of two or three) than the external forces acting to perturb the orbit. Due to this low nonvarying thrust, the hydrazine engine propulsion models described in Sections 2.4 and 2.5 are not valid for the ion engines. Instead, a method which computes the change in orbital elements caused by continuous low-level thrusting over an extended period time is required. Similar to the method used for the hydrazine engines this computational method

subdivides the maneuvers into incremental time segments of Δt duration. Computed velocity and position increments are vectorially added to the position and velocity vectors read from the initial orbit source at each computational time step. As a result, the firing of ion engines is treated as another perturbation of the original orbit. To compute the velocity and position increments, the following recursive formulas are used:

$$\begin{aligned} \Delta V_x &= \Delta V_x + KF_x \\ \Delta V_y &= \Delta V_y + KF_y \\ \Delta V_z &= \Delta V_z + KF_z \end{aligned} \tag{2-62}$$

$$\begin{aligned} \Delta X &= \Delta X + \left(\Delta V_x - \frac{1}{2} KF_x\right)\Delta t \\ \Delta Y &= \Delta Y + \left(\Delta V_y - \frac{1}{2} KF_y\right)\Delta t \\ \Delta Z &= \Delta Z + \left(\Delta V_z - \frac{1}{2} KF_z\right)\Delta t \end{aligned} \tag{2-63}$$

where ΔV_x, ΔV_y, ΔV_z = velocity increments (ERU per second)

ΔX, ΔY, ΔZ = position increments (ERU)

F_x, F_y, F_z = thrust components obtained by multiplying the unit thrust vector (as computed in Section 2.2) by the constant ion engine thrust level

K = value of $\Delta t/M$ (seconds per slugs)

Δt = incremental time step (seconds)

M = mass of the spacecraft (slugs)

$$M = W_I - \frac{T_{ION}}{ISP_{ION}} x\Delta t \tag{2-64}$$

where M = mass of the spacecraft (slugs)

W_I = weight of spacecraft at start of maneuver (pounds)

T_{ION} = thrust of the ion engine (0.001 pound)

ISP_{ION} = specific impulse of the ion engine (2500 seconds)

x = number of time steps since ignition time

Δt = incremental time step (seconds)

The equations are used recursively as follows:

At t = ignition time + Δt

$$\Delta V_1 = 0 + \frac{\Delta t}{M} F = \frac{F}{M} \Delta t$$

$$\Delta X_1 = 0 + \left(\Delta V - \frac{1}{2} \frac{\Delta t}{M} F \right) \Delta t = \frac{1}{2} \frac{F}{M} \Delta t^2$$

Substituting the equation $F = Ma$, one obtains

$$\Delta V_1 = a \Delta t$$

$$\Delta X_1 = \frac{1}{2} a \Delta t^2$$

At t = ignition time + $2 \Delta t$

$$\Delta V_2 = \Delta V_1 + \frac{\Delta t}{M} F = \frac{F}{M} (2 \Delta t)$$

$$\Delta X_2 = \Delta X_1 + \left(\Delta V_2 - \frac{1}{2} \frac{\Delta t}{M} F \right) \Delta t = \frac{1}{2} \frac{F}{M} (2 \Delta t)^2$$

Substituting the equation $F = Ma$ and setting $2\Delta t = \Delta t_{TOTAL}$, one obtains

$$\Delta V_2 = a\,\Delta t_{TOTAL}$$

$$\Delta X_2 = \frac{1}{2} a\,\Delta t^2_{TOTAL}$$

Applying the same analysis to any other time (ignition time + x Δt), one obtains

$$\Delta V_x = a\,\Delta t_{TOTAL}$$

$$\Delta X_x = \frac{1}{2} a\,\Delta t^2_{TOTAL}$$

where ΔV_x = incremental ΔV to be added to velocity vector at time x

ΔX_x = incremental change in position to be added to position vector at time x

a = acceleration due to thrusting

Δt_{TOTAL} = total incremental time ($x\Delta t$)

At each time step, the equations reduce to the standard set of velocity and position equations in a constant acceleration field. Also at each time step, the calculated position and velocity increments are added vectorially to the position and velocity vectors from the specified orbit source. The inertial orbital elements (Cartesian) formed are then converted to osculating Keplerian elements as described in Section 2.1.5. The converted osculating Keplerian elements form the burnout elements from thrusting with the ion engines for ΔT seconds. Note that the required thrust and ISP parameters are stored internally in CNTRLF (see Section 2.4.3).

2.7 ORBIT SOURCES BEFORE THE BURN

CNTRLF obtains its initial inertial position and velocity vectors (converted to osculating Keplerian elements) before a burn by reading the standard ephemeris sources available at GSFC. If these are not available, CNTRLF can propagate an orbit using the internal analytic generator BPACKT. The values read or propagated are used to determine the initial orbital elements (both osculating Keplerian and inertial position and velocity vector) at ignition time. These elements are used by the finite burn integrator (see Section 2.5) and also by the drift rate algorithm in calculating the initial drift rate (see Section 2.3.1.1). The initial orbit source is also used for all ion engine calculations (see Section 2.6). When the orbit source is external to CNTRLF, it resides either on a tape or on a disk and is in the form of an EPHEM file, ORB1 file, or GTDS ORBIT file.

2.7.1 Internal Orbit Source

CNTRLF contains an analytic propagator based on Brouwer theory (Reference 10). The internal generator is subroutine BPACKT. This subroutine serves as an executive routine to the standard ATS subroutine BPACKC (Reference 5). The propagator models the zonal and tesseral spherical harmonic terms which are used to describe variations in the Earth's gravitational field. Not included are the important Sun and Moon gravitational perturbations. If none of the standard orbit sources at GSFC is available, the internal generator can serve as the initial orbit source. In this mode the user enters known epoch elements at a given epoch time. The elements are either Keplerian osculating elements, injection elements, or inertial position and velocity vectors (see Section 2.1). The input elements are converted to osculating Keplerian elements and then to Brouwer mean elements. The Brouwer mean elements are used to propagate to spacecraft orbit to some arbitrary time after or before epoch. The mean elements are then converted back into osculating Keplerian elements. The primary purpose for the internal

generator is to calculate the drift rate after thrusting has started (see Section 2.3.1.1). It is used in the drift rate calculation regardless of the initial orbit source.

2.7.2 Standard Orbit Sources at GSFC

At GSFC there are two large scale orbit determination systems: GTDS (Reference 11) and the Definitive Orbit Determination System (DODS) (Reference 12). GTDS produces as output EPHEM files, ORB1 files, and GTDS ORBIT files. DODS has only the EPHEM and ORB1 capacity. The EPHEM and ORB1 files are sequential data sets containing epoch data and orbital position and velocity elements in the form of vector. Note that EPHEM and ORB1 files contain essentially the same information with different units. The GTDS ORBIT file is a direct-access data set which can contain the trajectories of multiple orbits. The user specifies which orbit is of interest through a level parameter. The data records in the file are read and interpolated using standard subroutines available for this purpose (Reference 13). In general, after tracking ATS-6 for 24 hours, the range and range rate data obtained are reduced into an orbit by the orbit computation engineer using either GTDS or DODS. Once an orbit has been determined, it is propagated over a month's span and the results are output as one of the files described above. Using the standard subroutines, CNTRLF reads the header record which contains epoch information and the appropriate data record which contains the position and velocity vector at ignition time. If the vectors at the desired time are not contained within the file or if there is an error in reading the file, the epoch information read is then used to initialize the internal orbit generator. In this case, an error message is printed and the internal orbit generator is automatically used as the initial orbit source.

APPENDIX A - ATS-6 HYDRAZINE PROPULSION SYSTEM DATA

A necessary step in the development of the ATS-6 orbital maneuver control program (CNTRLF) is the acquisition and incorporation in the program of a data set which accurately defines the thrust and specific impulse of the hydrazine thrusters as a function of propellant pressure and temperature. On October 12, 1972, the author visited Fairchild Industries and met with the propulsion personnel. All data available at that time including the prototype system test data was provided. These data have been analyzed according to the following criteria:

- Establishing the most appropriate format for utilization of the flight system data when these data become available
- Establishing ground rules for math models of the hydrazine system in the CNTRLF program

The analysis is summarized below together with the results, conclusions, and recommendations made on the basis of these findings.

A.1 PURPOSE OF ANALYSIS

The purpose of the analysis was to determine the most appropriate format for using the test data. This will establish ground rules for modeling the hydrazine thruster performance. Consideration was given to the following questions:

1. Which test data should be used?
   a. Individual thruster performance data
   b. System test data
   c. Both types of data

2. How should the data be used?

   a. Average all thrusters using a calibration factor to discriminate between thrusters

   b. Model each thruster individually

3. What thrust and ISP models are dictated by the data?

   a. Time and pressure dependency

   b. Temperature dependency

   c. A combination of the above

A.2 DATA USED

The type of tests and the data used in each follow.

1. Performance Mapping Tests--Each thruster was tested at a matrix of selected inlet temperatures and tank pressures. The thruster burn time was either 200 or 300 seconds for steady state thrusting. Necessary data were taken to allow thrust computation.

2. Individual Thruster Tests--Each thruster was tested at a constant inlet temperature of $70^{\circ}F$ and varying tank pressures. The burn time of the thruster was 200 seconds. Necessary data were taken to allow both ISP and thrust computation.

3. ATS-6 Sustained Firing Tests--One time engine tests were made of thrust and ISP at 1-, 6-, and 12-hour operating times. The inlet temperature and tank pressure were held constant.

All tests were conducted so that the calculation error in ISP and thrust would be less than ± 5 percent.

A.3 TESTING CONDITIONS

Pressure and temperature was read from a strip chart or, if they varied rapidly, an oscillograph was used. Calibration factors corrected equipment biases. In steady state flow the thrust was calculated from the test data by

$$T = P_c A_{tc} C_f$$

where T = the thrust in pounds

P_c = the measured chamber pressure. It is converted from PSIG to PSIA. An assumption is that tank pressure is a monotonicly increasing function of chamber pressure

A_{tc} = measured thrust area corrected for thermal expansion (inches^2)

C_f = thrust constant to be determined by the project office. One way of obtaining C_f is as follows:

Another expression for thrust, T, is

$$T = \delta A_{tc} C^2$$

where δ = propellant density

C = exit velocity

Thus

$$P_c A_{tc} C_f = \delta A_{tc} C^2$$

which reduces to

$$C^2 = \frac{P_c C_f}{\delta}$$

knowing Bernoulli's Equation

$$C^2 = \frac{2P_c}{\delta}$$

it can be concluded $C_f \simeq 2$.

In tests like the individual thruster tests, propellant flow was measured by a sight glass allowing the following equations to be solved:

$$I_{SP} = \frac{T}{\dot{W}}$$

where ISP = the specific impulse in seconds

T = the thrust in pounds

$\dot{W}$ = the rate of weight flow in pounds per second

$$\dot{W} = \frac{\Delta h K \delta}{\Delta t}$$

where Δh = the sight glass deflection (centimeters)

K = the sight glass constant (in^3 per centimeter)

δ = the propellant density

Δt = the time between readings of the sight glass

A.4 ANALYSIS PERFORMED

To perform the analysis, the data were graphed with tolerance lines and average data lines drawn, when appropriate. The following illustrations were generated from these graphs to compare thruster performance:

Table A-1. Repeatability

Table A-2. Individual Thruster Modeling

Table A-3. Average Thruster Modeling

Table A-4. Comparison of Individual Thruster Modeling to Average Thruster Modeling

Table A-5. Error in Burn Time Due to Worst Cases

Table A-6. Final Calibration values

Figure A-1. Final Thruster Model at $70^{o}F$

Explanatory notes are presented with each of these illustrations.

A.5 CONCLUSIONS

The following conclusions were drawn from the tables.

1. Use all data. Both the individual thruster test data and the performance mapping data should be used in the thrusting model due to the good repeatability of the data.

2. Model a single thruster. By averaging all the data, a single thruster model can be developed. This model is no worse than the worst case when an individual thruster is modeled. The model will give from 3 to 4 percent errors in burn time.

3. Use calibration factors with the model. The individual modeling shows on the average a 1 percent improvement over the average

modeling. Calibration factors will result in a similar improvement. The calibration factor will take the following form:

$$T_X = (1 + C_f)\, T_{ave}$$

where T_X = the thrust for thruster X

C_f = the calibration factor/100

T_{ave} = the average value of thrust for a homogeneous model

4. Model thrust and ISP as a function of time, pressure and inlet temperature. Although the data is not extremely sensitive to time and inlet temperature, provisions will be left in the program for time- and temperature-dependent data. The above conclusion is based on the following:

   a. Pulse shape is not important. For 400-second burns the error in not modeling pulse shape is between 0.005 and 0.09 percent.

   b. Thrust varies very little over time. At one hour, a 0.04 percent error is introduced by not modeling data as time-dependent. At twelve hours, the error only grows to 0.35 percent.

   c. Inlet temperature variations are within data spread. No trends could be seen with the data taken at different temperature during the performance mapping tests.

Table A-1. Repeatability

To test the repeatability of the thrusters used for orbital control, data were taken at the beginning and the end of the performance mapping test and were compared. At these times the pressure and temperature were the same (364 PSIA, 70°F).

THRUSTER NUMBER	5	6	7	8	13	14	15	16
THRUST AT BEGINNING OF TEST	0.1225	0.1240	0.1225	0.1245	0.1200	0.1265	0.1260	0.1230
THRUST AT END OF TEST	0.1245	0.1260	0.1295	0.1255	0.1190	0.1275	0.1260	0.1215
% CHANGE	1.7%	1.6%	4.4%	0.8%	0.8%	0.8%	0%	0.4%

NOTE: HIGHEST PERCENTAGE CHANGE WAS 4.4 PERCENT.

Table A-2. Individual Thruster Modeling

The differences between the individual thruster test and the performance mapping test were used to develop the error that could be expected if each orbital thruster is modeled. Both high and low pressure points were taken (360 PSIA and 160 PSIA); all data were at $70^{\circ}F$.

THRUSTER NUMBER	5	6	7	8	13	14	15	16
INDIVIDUAL THRUSTER TEST								
160 PSIA	0.0595	0.0630	0.0615	0.0615	0.0590	0.0630	0.0615	0.0595
360 PSIA	0.1205	0.1240	0.1230	0.1235	0.1190	0.1265	0.1240	0.1200
PERFORMANCE MAPPING TEST								
160 PSIA	0.0625	0.0625	0.0625	0.0625	0.0595	0.0635	0.0615	0.0600
360 PSIA	0.1235	0.1250	0.1255	0.1250	0.1195	0.1265	0.1245	0.1200
% CHANGE								
160 PSIA	4.6%	0.8%	1.6%	1.6%	0.8%	0.8%	0%	0.8%
360 PSIA	2.5%	0.8%	2.0%	1.2%	0.4%	0%	0.4%	0%
AVERAGE	3.55%	0.8%	0.9%	1.4%	0.6%	0.4%	0.2%	0.4%

NOTE: HIGHEST PERCENTAGE CHANGE WAS 4.6 PERCENT. THIS IS VERY CLOSE TO THE HIGHEST PERCENTAGE CHANGE IN TABLE A-1.

Table A-3. Average Thruster Modeling

The average values of thrust were compared to the individual thruster test data and the performance mapping test data to develop an error that could be expected if an average thruster value is used. Both high and low pressure points were taken (360 PSIA and 160 PSIA); all data were at $70^{o}F$.

THRUSTER NUMBER	5	6	7	8	13	14	15	16
AVERAGE VALUE								
160 PSIA	0.0615	0.0615	0.0615	0.0615	0.0615	0.0615	0.0615	0.0615
360 PSIA	0.1215	0.1215	0.1215	0.1215	0.1215	0.1215	0.1215	0.1215
INDIVIDUAL THRUSTER TEST % CHANGE								
160 PSIA	3.3%	2.4%	0%	0%	4.1%	2.4%	0%	3.3%
360 PSIA	0.8%	2.1%	1.3%	1.7%	2.1%	4.0%	2.1%	1.3%
PERFORMANCE MAPPING TEST % CHANGE								
160 PSIA	1.6%	1.6%	1.6%	1.6%	3.3%	3.2%	0%	1.3%
360 PSIA	2.6%	2.8%	3.4%	2.8%	1.7%	4.0%	2.5%	1.3%
% CHANGE								
160 PSIA	2.45%	2.0%	0.8%	0.8%	3.7%	2.8%	0%	2.3%
360 PSIA	1.7%	2.45%	2.35%	2.25%	1.9%	4.0%	2.3%	1.3%
AVERAGE	2.075%	2.225%	1.575%	1.525%	2.8%	3.4%	1.15%	1.8%

NOTE: HIGHEST PERCENTAGE CHANGE WAS 4.1 PERCENT. THIS IS CLOSE TO THE HIGHEST PERCENTAGE CHANGE IN TABLE A-1.

Table A-4. Comparison of Individual Thruster Modeling to Average Thruster Modeling

THRUSTER NUMBER	5	6	7	8	13	14	15	16
ERROR IN INDIVIDUAL THRUSTER MODELING	3.55%	0.8%	0.9%	1.4%	0.6%	0.4%	0.2%	0.4%
ERROR IN AVERAGE THRUSTER MODELING	2.075%	2.225%	1.575%	1.525%	2.8%	3.4%	1.15%	1.8%
IMPROVEMENT IF INDIVIDUAL THRUSTER MODELING IS USED	−1.475%	1.425%	0.675%	0.125%	2.2%	3.0%	0.95%	1.4%

NOTE: THE AVERAGE IMPROVEMENT WAS 1.0375 PERCENT WHEN USING INDIVIDUAL THRUSTERS RATHER THAN AN AVERAGE THRUSTER.

Table A-5. Error in Burn Time Due to Worst Cases

Taking values from the worst individual thrusters and putting them into the rocket equation at both high and low pressure, the error in burn time due to the error in ISP and thrust is computed. In the rocket equation the spacecraft's weight was 3000 pounds with a ΔV of 0.533 feet per second (typical ΔV maneuver to be expected in stationkeeping maneuvers).

$$t_B \doteq \frac{WT\ ISP}{T}\left(1 - e^{\frac{-\Delta V}{g\ ISP}}\right)$$

where t_B = the burn time in seconds

WT = the weight of the spacecraft in pounds

ISP = the ISP either worst case or average in seconds

T = the thrust either worst case or average in pounds

ΔV = the change in velocity required in feet per second

	160 PSIA			360 PSIA		
	T	ISP	t_B	T	ISP	t_B
AVERAGE VALUE	0.0615	217	808.106	0.1215	223.5	409.026
WORST CASE	0.0595	208	835.269	0.1175	214.5	422.95
DIFFERENCE BETWEEN AVERAGE AND WORST CASE			27.163			13.924
ERROR IN BURN TIME			3.361%			3.404%

NOTE: THIS TABLE SHOWS THAT THE LARGEST ERROR IN COMPUTED BURN TIME USING AN AVERAGE THRUSTER WOULD BE APPROXIMATELY 3.5 PERCENT.

Table A-6. Final Calibration Values

The calibration values listed below describe the deviations of each individual thruster from the model. The effect of attitude thruster firings during an orbital maneuver is not included. For initial values of the calibration factor, this effect is neglected.

The calibration factor takes the following form:

$$T_x = (1 + C_f)\, T_{ave}$$

where T_x = the thrust for thruster x

C_f = the calibration factor/100

T_{ave} = the average thrust from the homogeneous model

The initial value is developed from the test data. After orbital maneuvers new calibration factors based on actual in flight thruster performance should be developed. The effect of attitude thrusting (approximately 1.5 percent) should also be added to each calibration factor.

THRUSTER NUMBER	CALIBRATION FACTOR C_f
5	0.084
6	0.78
7	1.4
8	0.084
13	−0.77
14	0.084
15	−1.2
16	−0.34

The following homogeneous model of the hydrazine thruster onboard ATS-6 was developed from the test data:

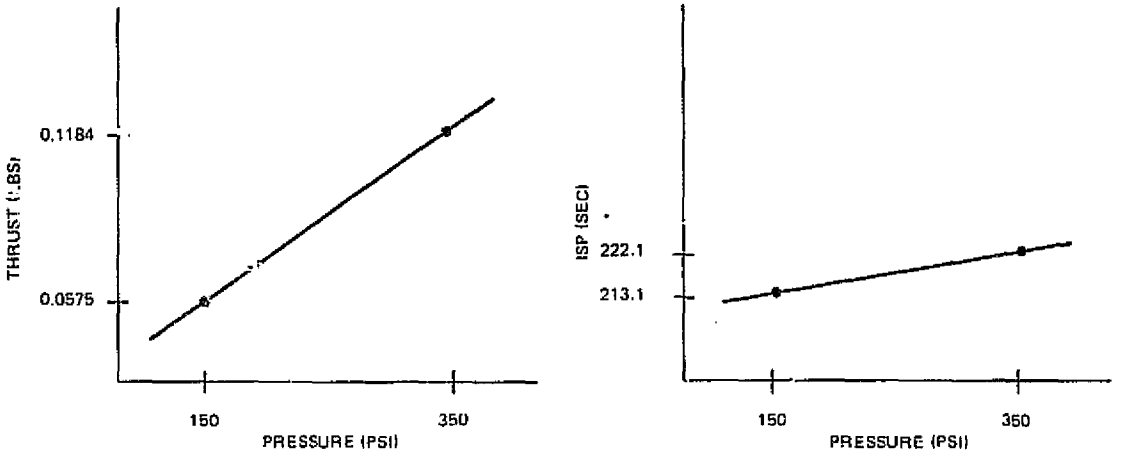

Figure A-1(a). As a Function of Pressure

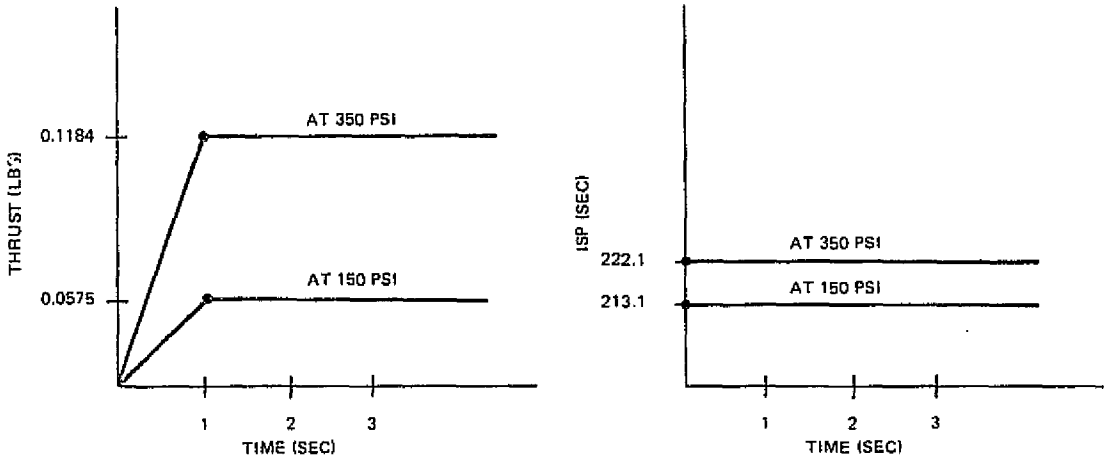

Figure A-1(b). As a Function of Time

Figure A-1. Final Thruster Model at $70^{O}F$

REFERENCES

1. Computer Sciences Corporation, 9101-05000-03TN, Mathematical and Programming Task Specification for the ATS-F Orbital Maneuver Control Program (CNTRLF), W. H. Comerford and C. E. Goorevich, August 1972

2. --, CSC/SD-75/6019, Applications Technology Satellite-F (ATS-F) Orbital Maneuver Control Program (CNTRLF) Description, C. E. Goorevich, June 1975

3. --, 3000-02700-01TM, User's Manual for the ATS-F Orbital Maneuver Control Program (CNTRLF), C. E. Goorevich, March 1973

4. --, 3000-30300-01TM, Subroutine Description for the Synchronous Meteorological Satellite Maneuver Control (SMSMAN) Program, A. B. Rochkind, February 1975

5. International Business Machines Corporation, Federal Systems Division, Applications Technology Satellite Programming System, Volumes I and II, May 1969

6. A. E. Roy, The Foundations of Astrodynamics. New York: MacMillan Company, 1965

7. Computer Sciences Corporation, CSC/SD-75/6017, Functional and Mathematical Specifications for the Applications Technology Satellite-F (ATS-F) Acquisition Prediction Program (FACTBL), D. C. Haley, June 1975

8. F. R. Moulton, An Introduction to Celestial Mechanics. New York: MacMillan Company, 1914

9. W. M. Kaula, Theory of Satellite Geodesy. Waltham: Blandell Publishing Company, 1966

10. Goddard Space Flight Center, X-643-68-131, Combined Solution for Low Degree Longitude Harmonics of Gravity From 12- and 24-Hour Satellites, C. A. Wagner, April 1968

11. Computer Sciences Corporation, 3000-03700-08TN, Brouwer Generator With Tesseral Acceleration Model (BPACKT), C. E. Goorevich, January 1974

12. International Business Machines Corporation, Federal Systems Division, Definitive Orbit Determination System User's Guide, Volumes I and II, March 1969

13. Computer Sciences Corporation, CSC/SD-75/6005, Goddard Trajectory Determination System User's Guide, E. L. Zavaleta, et al., April 1975

14. --, 5035-02700-02TM, Draft Material for the System Description and Operating Guide of the Flight Dynamics Support System, J. E. Dunn, 1972